

Abstracts

J. Miner. Stoffwechs. Muskuloskelet. Erkrank.
<https://doi.org/10.1007/s41970-022-00205-w>
© The Author(s), under exclusive licence to
Springer-Verlag GmbH Austria, ein Teil von
Springer Nature 2022



Jahrestagung der Österreichischen Gesellschaft für Rheumatologie & Rehabilitation

3.–5. November 2022

1 Pathophysiologie

1.1

The synovial cytokine milieu shapes synovial pathotypes in rheumatoid arthritis patients via synovial fibroblast–T-cell interactions

Kugler M¹, Dellinger M¹, Kartnig F^{2,1}, Müller L¹, Preglej T¹, Heinz L¹, Kiener H¹, Steiner G¹, Aletaha D¹, Tosevska A¹, Karonitsch T¹, Bonelli M¹

¹Medizinische Universität Wien, Abteilung für Rheumatologie, Wien, Austria;

²CeMM Research Center for Molecular Medicine, ÖAW, Wien, Austria

Introduction: Rheumatoid Arthritis (RA) is a chronic inflammatory disease, which is characterized by synovial inflammation resulting in bone and cartilage destruction. Crosstalk between activated fibroblast-like synoviocytes (FLS) and immune cells, such as CD4+ T cells, within the synovium might amplify synovial inflammation and joint destruction. In this study, the interaction profile of activated FLS and CD4+ T cells within an inflammatory setting and its consequence on synovial inflammation is elucidated.

Methods: To screen for factors that activate FLS in RA, isolated FLS were treated with different inflammatory cytokines and transcriptomic changes were measured with RNA-seq. Fluorescence activated cell sorting (FACS) purified naïve CD4+ T-cells from the same patients were co-cultured with the cytokine pre-treated FLS. Automated fluorescence microscopy and downstream bioinformatic image analysis allowed visualization and quantification of cell-cell interactions. After co-culture T-cells were isolated and T-cell activation, proliferation and differentiation was determined by flow cytometry.

Results: To model the in vivo situation, FLS were pre-stimulated with different pro- and anti-inflammatory cytokines. RNA-seq revealed cytokine specific activation patterns of FLS. Correspondingly, we observed distinct CD4+ T cells–FLS interaction profiles depending on the cytokine used for FLS activation. In line with distinct interaction profiles, specific patterns in CD4+ T cells activation, proliferation and differentiation of naïve T cells into CD62Lhigh CD45ROhigh memory T cells could be detected. Signatures of cytokine-stimulated FLS could be identified in transcriptomic data from synovial tissue samples.

Conclusion: Within this study, we highlight the role of FLS in orchestrating inflammation-associated synovial tissue remodeling and how cytokine induced CD4+ T cells–FLS interactions impact on T cell development.

1.2

STAT1 and STAT3 activation distinguishes psoriasis arthritis patients in active and inactive disease

Dreo B¹, Pietsch DR¹, Husic R¹, Lackner A¹, Fessler J², Rupp J¹, Muralikrishnan AS¹, Thiel J¹, Stradner MH¹, Bosch P¹

¹Klinische Abteilung für Rheumatologie und Immunologie, Graz, Austria;

²Klinische Abteilung für Pathologie und Immunologie, Graz, Austria

Introduction: Numerous cytokines that influence disease activity in psoriatic arthritis (PsA) are modulators of the Janus Kinases/Signal Transducers and Activators of Transcription (JAK/STAT) pathway. The JAK1/STAT1/STAT3/STAT5 network can drive the expansion of Th17 and regulatory T cells via proinflammatory cytokines in PsA joints [1, 2], while hyperphosphorylation of STAT3 in immune cells has previously been shown to promote PsA pathogenesis through the Interleukin (IL)-23/IL-17/IL-22 axis [3]. Therefore, the phosphorylation status of STAT molecules in leucocytes of PsA patients may indicate active disease and could potentially guide treatment with JAK inhibitors. Thus, the aim of this study was to analyse phosphorylated STAT (pSTAT) levels of circulating leucocyte subsets in PsA patients with active and inactive disease.

Methods: Whole blood was drawn on consecutive PsA patients fulfilling the CASPAR criteria[4] to perform flow cytometry analysis using the BD FACSLyric platform. Disease activity was assessed using the Disease activity for psoriasis arthritis (DAPSA) score [5]. All steps from storage of drawn blood to cell fixation were performed at 4 °C to prevent auto-activation of leucocytes. The geometric mean fluorescence intensities (gMFI) of pSTATs in granulocytes, monocytes, B cells and CD4+/- naïve/memory T cells were compared between patients with moderate to high (MoDA/HDA) and remission to low disease activity (REM/LDA). Correlation analysis between gMFIs and DAPSA scores were performed.

Results: 42 patients (female ratio: 0.48) with established PsA (median ± standard deviation, age: 56 ± 12.54 years, disease duration: 8.50 ± 7.10 years) were included in this study. 21% of patients were in MoDA/HDA, while the remaining 79% were in REM/LDA. Patients in MoDA/HDA showed significantly higher pSTAT3 levels in CD4+ naïve (gMFI median ± standard deviation: 284.5 ± 79.9 vs 238 ± 92.9, $p = 0.011$), CD4- naïve (297 ± 107.5 vs 238 ± 98.4, $p = 0.04$), CD4+ memory (227 ± 62.9 vs 190.5 ± 72.2, $p = 0.009$) and CD4- memory T cells (209 ± 66.8 vs 167.0 ± 64.9, $p = 0.036$). On the other hand, PsA patients in remission or low disease activity displayed higher pSTAT1 levels in granulocytes (2509 ± 1887 vs 1330.5 ± 784.1, $p = 0.040$) and monocytes (255 ± 230 vs 144 ± 62.5, $p = 0.049$). Positive correlations were found between DAPSA scores and pSTAT3 in CD4+ naïve and memory T cells (Spearman's correlation coefficient rho (ρ) = 0.5, $p = 0.0012$ and $\rho = 0.47$, $p = 0.0025$ resp.) whereas pSTAT1 in granulocytes and monocytes were negatively correlated with the DAPSA scores ($\rho = -0.45$, $p = 0.0074$ and $\rho = -0.34$, $p = 0.05$).

Conclusion: Differential phosphorylation of STAT3 and STAT1 molecules in circulating leucocyte subsets indicates PsA disease activity. Further

Abstracts

studies to examine the value of STAT phosphorylation patterns guiding JAK inhibitor therapy are underway.

References

1. Fiocco U et al (2015) Ex vivo signaling protein mapping in T lymphocytes in the psoriatic arthritis joints. *J Rheumatol* 93:48–52. <https://doi.org/10.3899/jrheum.150636>
2. Raychaudhuri SK, Abria C, Raychaudhuri SP (2017) Regulatory role of the JAK STAT kinase signalling system on the IL-23/IL-17 cytokine axis in psoriatic arthritis. *Ann Rheum Dis* 76(10):e36–e36
3. Calautti E, Avalle L, Poli V (2018) Psoriasis: A STAT3-centric view. *IJMS* 19:6. <https://doi.org/10.3390/ijms19010171>
4. Taylor W, Gladman D, Helliwell P, Marchesoni A, Mease P, Mielants H (2006) Classification criteria for psoriatic arthritis: Development of new criteria from a large international study. *Arthritis Rheum* 54(8):2665–2673. <https://doi.org/10.1002/art.21972>
5. Schoels MM, Aletaha D, Alasti F, Smolen JS (2016) Disease activity in psoriatic arthritis (PsA): Defining remission and treatment success using the DAPSA score. *Ann Rheum Dis* 75(5):811–818. <https://doi.org/10.1136/annrheumdis-2015-207507>

1.3

Distinctive STAT activation patterns subgroup rheumatoid arthritis patients in active disease

Dreo B¹, Muralikrishnan AS¹, Husic R¹, Fessler J², Lackner A¹, Bosch P¹, Rupp J¹, Buchmann A³, Khalil M³, Thiel J¹, Stradner MH¹

¹Klinische Abteilung für Rheumatologie und Immunologie, Graz, Austria;

²Klinische Abteilung für Pathologie und Immunologie, Graz, Austria;

³Klinische Abteilung für Neurologie, Medizinische Universität Graz, Austria

Introduction: In Rheumatoid Arthritis (RA) an imbalance of pro- and anti-inflammatory cytokines and the subsequent activation of the JAK/STAT pathway are hallmarks of disease pathogenesis and progression. Thus, many therapeutic approaches in RA target cytokines, their respective receptors or downstream signaling molecules. If chronically elevated cytokine levels in vivo, however, affect downstream cellular signaling is not well understood. Thus, the aim of this study was to assess the cytokine milieu and downstream activation of STATs in peripheral blood leucocytes of RA patients.

Methods: Whole blood was drawn from 62 consecutive RA patients fulfilling the 2010 EULAR/ACR criteria (median + standard deviation, female ratio: 0.77, age: 64 ± 13 years). Nine healthy controls (HC, female ratio: 0.78, age: 48 ± 5 years) served as control group. Serum interferon gamma (IFN γ), interleukin (IL)-6, IL-10, IL-12p70, IL-17A and tumor necrosis factor alpha (TNF α) concentrations were measured using a highly sensitive single molecule array (SIMOA). Assessment of phosphorylated (*p*)-STAT levels in granulocytes monocytes, B and T-cells was performed by flow cytometry. Geometric mean fluorescence intensities (gMFIs) of pSTAT1/3/5a,b/6 were used as indicators for JAK/STAT pathway activation.

Results: Serum cytokine levels of IFN γ , IL-6, IL-10, IL-17A and TNF α were significantly elevated in RA patients compared to HCs and positively correlated with disease activity (all $p \leq 0.05$). 28/62 RA patients had moderate or high disease activity (MHDA). Unsupervised hierarchical clustering showed that 20/28 MHDA RA patients shared a profile of increased cytokines. In contrast, 8/28 patients showed no increase in cytokine levels. Measurement of pSTAT levels revealed that pSTAT1/3 and -6 levels in monocytes, granulocytes and T-cells were elevated in HCs but diminished in RA patients. Moreover, pSTAT6 levels of various leucocytes negatively correlated with cytokine levels. Stratification models of MHDA RA patients identified 6 patients with low cytokine and pSTAT levels, 9 patients with high cytokine concentrations but no subsequent STAT activation and 11/28 high-profile patients with both elevated cytokine and pSTAT levels. **Conclusion:** Here we describe a heterogeneity of serum cytokine milieu and downstream STAT activation in RA patients. We suggest that this observation might predict treatment success of JAK/STAT inhibitors, but further studies are needed for validation.

1.4

Deep immune phenotyping of SLE and RA by machine learning

Prietl B^{1,2}, Vera-Ramos J², Herbstrofer L¹, Pfeifer V^{1,2}, Lopez-Garcia P², Brezinsek H², Pieber T^{2,1}, Stradner M²

¹Center for Biomarker Research in Medicine, Graz, Austria; ²Medizinische Universität Graz, Graz, Austria

Introduction: Breakdown of self-tolerance is an important common mechanism in autoimmunity. Despite considerable clinical heterogeneity, many autoimmune diseases exhibit common immunological mechanisms leading to a breakdown of self-tolerance. Identification of unique and similar patterns across different autoimmune disease may help to understand their pathophysiology behind. Establishing workflows for the multi-parameter deep immune phenotyping of T- and B-cells by unsupervised machine learning (ML) methods for feature extraction, cluster analysis and anomaly detection.

Methods: We use machine learning to identify common patterns and dissimilarities between type 1 diabetes (T1D, $n=69$), rheumatoid arthritis (RA, $n=63$), systemic lupus erythematosus (SLE, $n=38$) and healthy controls ($n=69$) samples based on multi-plex immune phenotyping. PBMCs were isolated from patients with T1D, RA, SLE, and controls. A flow cytometry-based approach was applied, and a traditional analysis was compared to a ML method implemented in R [1] and based on self-organizing maps. Our pipeline includes unsupervised pre-gating, normalization, FlowSOM clustering [2], and a statistical model (GLMM), to check for significant differential abundances of cell populations among the autoimmune conditions.

Results: After applying our automated workflow to one T cell panel we could identify 14 cell clusters present in all the samples. The GLMM test revealed a cluster with a significant difference ($p=0.035$) and a trending one ($p=0.059$) on the abundance across the different diseases. In particular, CD4pos T cells expressing high IL-7 receptor (CD127) levels and median amounts of CD15s but low CD25, CD161 and FoxP3 are increased in T1D whereas CD4+CD25++CD15s+FoxP3lowCD161lowCD45RA- cells are increased in SLE.

Conclusion: This unbiased, unsupervised ML workflow was able to identify canonical and novel clusters of T cells that are similar in RA, SLE and T1D. Additionally, a novel memory T cell population expressing CD15s was shown. This unsupervised analysis approach for large datasets enables the discovery of new immune cell populations complementing traditional workflows.

References

1. Ellis B, Haaland P, Hahne F, Le Meur N, Gopalakrishnan N, Spidlen J, Jiang M, Finak G (2021) flowCore: flowCore: Basic structures for flow cytometry data. R package version 2.6.0
2. Van Gassen S, Callebaut B, Van Helden MJ, Lambrecht BN, Demeester P, Dhaene T, Saeyens Y (2015) FlowSOM: Using self-organizing maps for visualization and interpretation of cytometry data. *Cytom Part A* 87(7):636–645

1.5

Expression of co-stimulation marker CD19 on b cells is not altered by rituximab intake in patients suffering from systemic sclerosis

Dreo B¹, Prietl B², Kofler S², Pfeifer V², Sourij H³, Moazedi-Fürst F¹, Zenz S¹, D’Orazio M¹, Kreuzer S¹, Thiel J¹, Stradner MH¹, Brezinsek H¹

¹Klinische Abteilung für Rheumatologie und Immunologie, Graz, Austria;

²CBmed GmbH—Center for Biomarker Research in Medicine, Graz, Austria;

³Klinische Abteilung für Endokrinologie und Diabetologie, Graz, Austria

Introduction: CD19 is a membrane glycoprotein interacting with different surface molecules like the B cell receptor (BCR) and is crucial for antigen-independent development as well as immunoglobulin-induced activation of B cells [1]. Alterations in this signalling pathway can incline autoantibody production and systemic autoimmunity in humans. Rituximab (RTX), a CD20 antagonist appears to be an effective candidate in the treatment of different autoimmune diseases that are partly driven by autoreactive B cells, such as systemic sclerosis (SSc) [2]. It has been specu-

lated that RTX might work not only by depleting B cells but also to down regulate activation markers, such as CD19. Thus, this study aimed to give an in-depth analysis of CD19 abundance and activation on B cells in SSc patients with and without RTX treatment.

Methods: Peripheral blood samples from 41 patients suffering from SSc (median \pm standard deviation SD, age: 54.3 ± 10.6 years, female ratio: 0.8) and 45 age- and sex-matched healthy controls (HC) (age: 51.0 ± 13.9 years, female ratio: 0.8) were drawn and PBMCs were isolated on-site. We performed flow cytometry analysis on a standardized BD LSRFortessa platform to identify B cell (CD19+CD20+) subpopulations. The geometric mean fluorescence intensity (gMFI) for CD19 in all B cell subtypes was extracted from the data set and used for further statistical analysis. Additionally, a quantitative flow cytometric bead-based assay (QuantiBRITE PE kit from Becton Dickinson) was used for the estimation of CD19 antibodies bound per cell.

Results: 3 SSc patients were in high disease activity at the time of blood drawal. 23 patients were under RTX therapy of whom 5 patients still displayed measurable B cells frequencies. Naïve B cells made up the most abundant B cell population in SSc patients. The frequency of IgM+/IgD+/CD27- B cells was $67.9\% \pm 13.2$ (mean \pm SD), followed by class-switched memory (IgM-/IgD-/CD27+, 10.5 ± 4.9), non-switched memory B cells (IgM+/IgD+/CD27+, 4.0 ± 3.6) and plasmablasts (0.3 ± 4.4). Pairwise Wilcoxon Tests (Bonferroni-corrected for multiple testing) showed significant differences ($p < 0.001$) between frequencies of naïve B cells and all other cell types. In contrast, naïve B cells displayed the second lowest CD19 gMFI levels (7601.0 ± 1912.0). Non-switched memory B cells in SSc patients showed the highest CD19 gMFI ($10,620.0 \pm 15,689.8$), followed by class-switched B cells (9388 ± 3048.6). Plasmablasts displayed the lowest CD19 gMFI levels (4799.0 ± 4185.7). This trajectory in decreasing CD19 gMFI was found in both HCs and SSc patients. We saw a significant reduction in percentages of non-switch B cells and class-switched B cells in SSc patients compared to HCs (4.0 ± 3.6 vs 6.5 ± 4.2 , $p = 0.029$, 10.5 ± 4.9 vs 13.2 ± 7.2 , $p = 0.04$) but an increase in CD19 gMFI in nonswitched B cells (HC: 9204.5 ± 2116.8 , $p = 0.05$). SSc patients under RTX treatment had significantly lower class-switched memory B cell frequencies compared to HCs $p = 0.015$. RTX did not affect CD19 gMFI or bound CD19 in SSc.

Conclusion: RTX treatment in SSc is not associated with downregulation of the co-stimulation marker CD19. Thus, the main effect of this drug is the reduction of B cells, especially class-switched memory B cells that might have a high capacity to activate other cells involved in the pathogenesis of SSc.

References

- Wang M et al (2019) Identification and Validation of Predictive Biomarkers to CD19- and BCMA-Specific CART-Cell Responses in CART-Cell Precursors. *Blood* 134(1):622–622. <https://doi.org/10.1182/blood-2019-122513>
- Ebara S et al (2021) Safety and efficacy of rituximab in systemic sclerosis (DESIRE): a doubleblind, investigator-initiated, randomised, placebo-controlled trial. *Lancet Rheumatol*. [https://doi.org/10.1016/S2665-9913\(22\)00131-X](https://doi.org/10.1016/S2665-9913(22)00131-X)

2 Klinische Studien und Präsentationen

2.1

Clinical, imaging and blood biomarkers to assess one-year progression risk in fibrotic interstitial lung diseases

Lang D^{1,2}, Shao G^{1,2}, Akbari K^{3,2}, Hintenberger R^{4,2}, Horner A^{1,2}, Lamprecht B^{1,2}

¹Department of Internal Medicine 4, Kepler University Hospital, Linz, Austria;

²Johannes Kepler University Linz, Medical Faculty, Linz, Austria; ³Central Radiology Institute, Kepler University Hospital, Linz, Austria; ⁴Department of Internal Medicine 2, Kepler University Hospital, Linz, Austria

Introduction: We aimed to evaluate biomarkers derived from baseline patient characteristics, computed tomography (CT) and peripheral blood for prognosis of disease progression in fibrotic ILD patients.

Methods: Of 209 subsequent ILD-board patients enregistered, 142 had complete follow-up information and were classified fibrotic ILD as defined by presence of reticulation or honeycombing. Most patients had been diagnosed with autoimmune-associated ILD (24%), followed by idiopathic NSIP (21%) and IPF (16%). Using a standardized semi-quantitative CT evaluation, typical ILD findings like honeycombing or ground glass opacities were added up in 6 defined lung fields. Progression at one year was defined as relative loss of $\geq 10\%$ in forced vital capacity, of $\geq 15\%$ in diffusion capacity for carbon monoxide, death, or lung transplant. Two thirds of the patients were randomly assigned to a derivation cohort evaluated for the impact of age, sex, baseline lung function, CT finding scores and blood biomarkers on disease progression. Significant variables were included into a logistic regression model, its results were used to derive a progression risk score which was then applied to the validation cohort.

Results: In the derivation cohort, age, monocyte count $\geq 0.65\text{G/L}$, honeycombing and traction bronchiectasis extent had significant impact. Multivariate analyses revealed the variables monocyte count $\geq 0.65\text{G/L}$ (1 point) and combined honeycombing or traction bronchiectasis score (0 vs. 1–4 (1 point) vs. 5–6 lung fields (2 points)) as significant, so these were used for score development. In the derivation cohort, resulting scores of 0, 1, 2 and 3 accounted for one-year progression rates of 20%, 25%, 46.9% and 88.9%, respectively. Similarly, in the validation cohort, progression at one year occurred in 0%, 23.8%, 53.9% and 62.5%, respectively, a score ≥ 2 showed 70.6% sensitivity and 67.9% specificity, receiver operating characteristic analysis for the scoring model had an area under the curve of 71.7%.

Conclusion: The extent of honeycombing and traction bronchiectasis, as well as elevated blood monocyte count predicted progression within one year in fibrotic ILD patients.

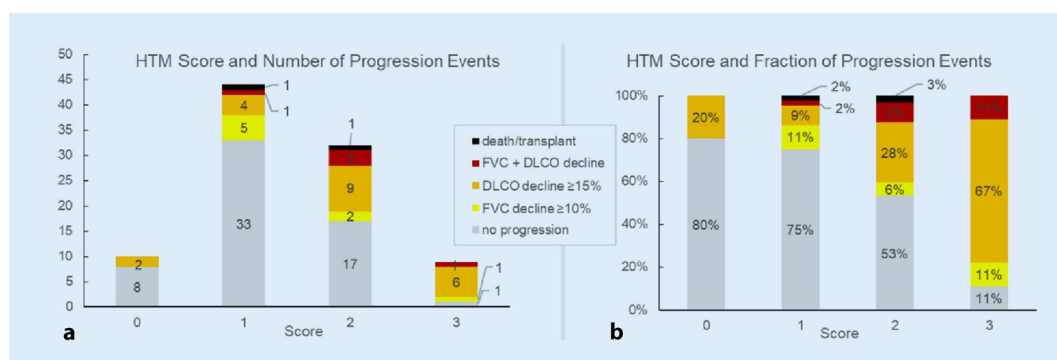


Fig. 1 | 2.1 ▲ HTM score with number (a) and fraction (b) of progression events in the derivation cohort ($n = 95$) (HTM honeycombing, traction bronchiectasis, monocyte, FVC forced vital capacity, DLCO diffusion capacity for carbon monoxide)

Abstracts

2.2

Altered cellular immune response to vaccination against SARS-CoV-2 in patients with B-cell depleting therapy

Hodl I, Sallegger C, Dreßler B, Lackner A, Moazedi-Fürst F, Thiel J, Stradner M, Fessler J

Medizinische Universität Graz, Graz, Austria

Introduction: B-cell depleting therapies result in diminished humoral immunity following vaccination against COVID-19, but our understanding on the impact on cellular immune responses is limited. Here, we performed a detailed analysis of cellular immunity following mRNA vaccination in patients receiving B-cell depleting therapy.

Methods: We analyzed T-cell responses in autoimmune patients treated with B-cell depleting therapy and healthy controls after mRNA vaccination against COVID-19. We isolated PBMCs and stimulated them with a peptide pool covering the spike protein in vitro. Reactive T-cells were determined by IFN γ ELISpot assay and staining for effector cytokines by flow cytometry. Anti-SARS-CoV-2 spike receptor-binding domain antibody assays were performed to elucidate B-cell responses. To complement our cellular analysis, we performed immunophenotyping for T- and B-cell subsets.

Results: In this work, we show that SARS-CoV-2 vaccination using mRNA vaccines elicits cellular T-cell responses in patients under B-cell depleting therapy. Some facets of this immune response including TNF α production of CD4+ T-cells and GzmB production of CD8+ T-cells, however, are distinctly diminished in these patients. Consequently, it appears that the finely coordinated process of T-cell activation with a uniform involvement of CD4+ and CD8+ T-cells as seen in HCs is disturbed in autoimmune patients. In addition, we observed that immune cell composition does impact cellular immune responses as well as sustainability of anti-spike antibody titers, a fact that also holds true for healthy individuals.

Conclusion: Our data suggest disturbed cellular immunity following mRNA vaccination in patients treated with B-cell depleting therapy. Immune cell composition may be an important determinant for vaccination efficacy.

2.3

Identifying individuals at risk for Sjögren's syndrome—The pre-Sjögren syndrome targeted immunology evaluation (PRESTIGE) study

Zenz S¹, Erlacher L¹, Windisch E¹, Dreßler B¹, Javorova P¹, Lackner A¹, D'Orazio M¹, Thiel J¹, Cornef D², Stradner M¹

¹Klinische Abteilung für Rheumatologie und Immunologie, Universitätsklinik für Innere Medizin, Medizinische Universität Graz, Graz, Austria; ²Klinische Abteilung für Rheumatologie, Universität von Brest, Brest, France

Introduction: Primary Sjögren's Syndrome (pSS) is a chronic autoimmune disease. Symptoms range from sicca to systemic, potentially life-threatening organ damage. Little is known about the onset of the disease. Anti-Ro antibodies are described to develop years before the first symptoms. In addition, first degree relatives of pSS patients have an 11- to 19-fold increased risk of developing pSS themselves. The aim of the study was to identify and follow-up individuals at risk for pSS in order to study symptoms and immune pathology before and at development of pSS.

Methods: In this ongoing long-term study individuals at risk for developing pSS but not fulfilling the ACR-EULAR classification criteria of pSS were included, defined as: (1.) Anti-SSA positive individuals (Anti-SSA+) without any sicca symptoms or diagnosis of an underlying systemic autoimmune disease; (2.) First degree relatives of patients (relatives) with an established diagnosis of pSS and typical autoantibodies (ANA \geq 1:160 and/or anti-SSA+ and/or rheumatoid factor+); (3.) Individuals with at least one feature of the ACR-EULAR classification criteria for pSS, but not fulfilling the criteria (incomplete). At baseline and at annual visits, demographic data, blood, saliva and urine samples were collected and stored. Salivary and lacrimal flow, salivary gland ultrasonography (SGUS), and patient-related outcome measures were analysed. A lip salivary gland biopsy was

performed at baseline and upon development of symptoms suggestive of pSS. The primary endpoint was the development of definite pSS according to the ACR-EULAR classification criteria.

Results: After the first year of recruitment, 50 individuals (Anti-SSA+ $n=27$, relatives $n=21$, incomplete $n=2$) were screened at baseline, of whom 28 were identified as individuals at risk for pSS and were included in the study. Twenty-two individuals were excluded from the study, most of whom were "relatives" with negative autoantibodies. Of these 28 individuals at risk, 89% were female ($n=25$), they had a median age of 53 years (IQR: 19) and 57% ($n=16$) had positive antinuclear antibodies. 86% were positive for anti-SSA and 14% were positive for anti-SSB. Decreased complement C3 and C4 were found in 18% and 4%, respectively. Serum IgG concentration was elevated in 29% of individuals. A reduction of lacrimal flow was found in 29% and stimulated whole salivary flow was reduced in 29%. The median of the ESSPRI was 1.6 (3.0). Eighteen percent of the investigated individuals had a pathological ultrasound [Hocevar score median 4.5 (9.0)] and in 9% a focus score ≥ 1 [median 0.15 (0.57)] was found in the lip salivary gland biopsies. Four patients (14%) met the primary endpoint and were diagnosed with pSS within the first year.

Conclusion: The design of the PRESTIGE study allows us to follow individuals at risk for pSS and will help to unveil symptoms and immune pathology as pSS develops. We suggest to establish a larger international pre-pSS cohort to increase statistical power.

2.4

Humoral immune response in rituximab treated patients following SARS-CoV2 vaccination

Storch K¹, Bécède M¹, Winkler S², Winkler F², Veitl M³, Sautner T⁴, Sautner J¹

¹2. Medizinische Abteilung, NÖ Kompetenzzentrum für Rheumatologie, Stockerau, Austria; ²Universitätsklinik für Innere Medizin I, AKH, Wien, Austria; ³Institut für chemische und medizinische Labordiagnostik, Krankenhaus der Barmherzigen Brüder, Wien, Austria; ⁴Ärztliche Direktion, Krankenhaus der Barmherzigen Brüder, Wien, Austria

Introduction: Rituximab (RTX) is a monoclonal antibody targeting CD20 and is known as a cornerstone in the management of haematological disorders and various inflammatory rheumatic diseases. B cell depleting therapy with RTX has an influence on humoral immune response following vaccination. Recent studies are already addressing the effect of a SARS CoV2-vaccination in patients on B-cell depleting therapies [1, 2]. The key question is as to whether RTX-treated patients can develop a humoral and T-cell-mediated immune response against SARS-CoV-2 following immunization.

Methods: The patient dataset was screened for patients under RTX treatment in various indications. Additionally, patients being considered for RTX treatment, were prioritized for SARS CoV2-immunization and enrolled. RTX treated patients ($n=17$) were vaccinated with the mRNA-1273

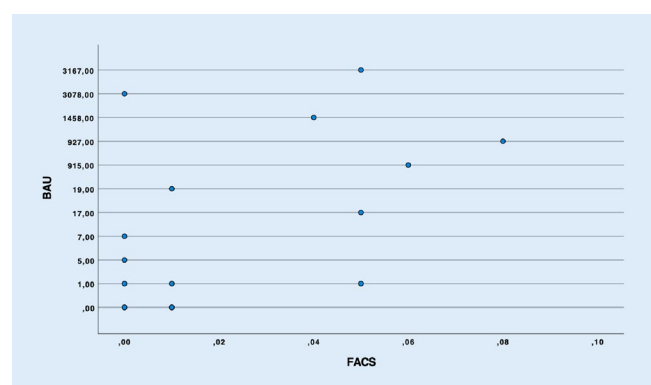


Fig. 1 | 2.4 ▲ There was a statistically significant correlation between the peripheral B cell count and SARS-CoV2 specific antibody levels <15 BAU/ml

vaccine (Moderna) sequentially, the first dosage in March 2021 following the second in April 2021. Four weeks after the second vaccination, serum samples were obtained to screen for antibodies against the receptor-binding domain (RBD-Cutoff BAU/ml<15), in addition a FACS analysis was carried out and the peripheral CD19+ B cells were determined. The last dosage of RTX was administered 3–9 months before immunization.

Results: All RTX treated patients ($n=17$) showed a peripheral CD19+ B cell count of $<0.1 \times 10^9/l$ 4 weeks after the 2nd vaccination. There was a statistically significant correlation between the peripheral B cell count and SARS-CoV2 specific antibody levels <15 BAU/ml (Fig. 1). There were no detectable peripheral CD19+ B cells in patients with RBD antibody levels <15 BAU/ml ($p=0.028$).

Conclusion: As confirmed in previous studies, in a cohort vaccinated with the mRNA-1273 vaccine, we could also show that patients without detectable CD19+ B cells did not develop specific SARS-CoV2 antibodies. Nevertheless, it is already known that RTX treated patients can build specific antibodies against SARS-CoV2 as soon as the peripheral CD19+ B cells partially repopulate, which should be investigated in more detail.

References

1. Mrak D, Tobudic S, Koblischke M et al (2021) Ann Rheum Dis 80:1345–1350
2. Bonelli MM, Mrak D, Perkmann T et al (2021) Ann Rheum Dis 80:1355–1356

2.5

First symptoms at the onset of primary Sjögren's syndrome—the patients' perspective of a sneaky disease

Lackner A¹, Fessler J¹, Zenz S¹, Hermann J¹, Thiel J², Stradner MH¹

¹Medizinische Universität Graz, Graz, Austria; ²Medizinische Universität Graz, Rheumatologie, Graz, Austria

Introduction: The aim of this study was to investigate patients' recollection of the first symptoms before diagnosis of PSS in qualitative interviews. The second aim was to verify and quantify these aspects in a representative cohort.

Methods: All PSS patients fulfilled the EULAR/ACR 2016 classification criteria. In the first part of the study, consecutive PSS patients were recruited for individual, semi-structured interviews. A discussion guide with five open-ended questions was developed to explore patients' experiences on the onset of PSS. All interviews were audio-recorded and transcribed verbatim, and an inductive thematic data analysis was performed using MAXQDA software (VERBI, Berlin, Germany). In the second part, the identified aspects of the qualitative analysis were grouped to a checklist with ten items. Patients were asked to complete the checklist before their routine clinical assessment.

Results: One-hundred and thirty-four patients participated in the study. The qualitative part was completed by 31 PSS patients; 90.3% ($n=28$) were female and patients had a mean disease duration of 6.9 years (± 5.7 (SD)) and a mean age of 58.1 years (± 12.6). Four different major aspects emerged of how patients experienced the beginning and first symptoms of PSS: (1) sicca symptoms started after initial swelling of parotis and/or lymph nodes (2) "Classic" PSS symptoms (fatigue, pain, dryness): patients reported wandering joint pain before diagnosis with a long time apart from first symptoms until diagnosis. Patients described joint pain, chronic malaise, and fatigue over months. (3) Hormonal changes (e.g. after birth, hysterectomy) or infections before the onset of PSS symptoms. (4) Slowly progressing discomfort due to sicca: patients reported a slow progression of symptoms with no initial recognition of sicca discomfort. In these patients recurrent dental problems and loss of teeth in the years prior to diagnosis was common. In the second part of the study, the four themes were verified in an independent cohort of 103 PSS patients. Patients were 59.9 (± 13.7) years old and six patients were male. The main symptom before diagnosis was dryness ($n=77$, 74.8%) with wandering joint pain ($n=51$, 49.5%) and fatigue ($n=47$, 45.6%). In 38.8% ($n=40$), patients reported a swelling/inflammation of the parotid gland at the onset of disease.

Conclusion: We identified four themes describing the initial symptoms of PSS. Raising awareness of these symptoms among physicians and among the general public may allow earlier diagnosis of PSS.

2.6

Defining an acceptable state of quality of life in primary Sjögren's syndrome

Lackner A¹, Sanz A², Zenz S¹, Hermann J¹, Thiel J², Stradner MH¹

¹Medizinische Universität Graz, Graz, Austria; ²Medizinische Universität Graz, Rheumatologie, Graz, Austria

Introduction: To define the threshold of an acceptable QoL state (AQLS) and the minimal detectable change (MDC) of the PSS-QoL.

Methods: Data of patients from the PSS registry fulfilling the 2016 ACR/EULAR classification criteria for PSS were analysed. Patients completed the PSS-QoL and ESSPRI (EULAR Sjögren's syndrome patient-reported index), disease activity was assessed by the ESSDAI (EULAR Sjögren's syndrome disease activity index) and an evaluator's global assessment (EGA, scale from 0–10). Receiver operating characteristic curve analyses were used to estimate the AQLS based on patients' assessment on the extent of HRQL. We selected the optimal cut-off of PSS-QoL by the maximal Youden index. At the follow-up visits after 12 months, patients assessed, whether their HRQL had changed. An anchoring method based on this evaluation was used to estimate the MDC of PSS-QoL. Furthermore, clinical data were compared in AQLS and non-AQLS groups.

Results: Data from 152 PSS patients were analysed of which of 91.4% ($n=139$) were female. The mean age was 59.65 ± 12.3 years (\pm standard deviation) and the mean disease duration was 5.6 ± 5.3 years. The AQLS estimate was defined as PSS-QoL ≤ 29.5 . 40.1% ($n=61$) were categorized to be in AQLS. Although AQLS patients were significantly younger (56.9 ± 13.1 years vs 61.5 ± 11.4 years, $p < 0.01$) they had a longer disease duration (6.9 ± 5.8 years vs. 4.7 ± 4.7 years, $p < 0.05$) compared to non-AQLS patients. AQLS patients had a lower EGA (2 [0–5] vs 3 [0–7], $p < 0.01$ (median [range])), higher IgG (15.7 [7.7–33.8, range] vs 13.1 [6.5–38.1], $p < 0.05$) and higher rheumatoid-factor IgA (84 [0–500] vs 20 [0–500], $p < 0.01$). AQLS patients showed significantly lower burden of sicca (measured by ESSPRI and sicca VAS scores). The MDC for PSS-QoL was defined as 12.2 points. After one year, patients' HRQL did not change in 83.3% and got worse 7.1%.

Conclusion: This study determined the AQLS and the minimal detectable change for HRQL. These results will help evaluating the HRQL of patients in clinical practice, as well as possible assistance designing future clinical trials. Patients in AQLS show lower dryness scores but higher immunological activity compared to non-AQLS patients. Longitudinal studies are needed to determine factors affecting patients' HRQL in PSS.

2.7

Prediction of ineffectiveness of biological drugs using machine learning and explainable AI methods

Ukalovic D¹, Leeb B², Rintelen B², Eichbauer-Sturm G⁴, Spellitz P⁶, Puchner R⁶, Herold M⁷, Stetter M⁸, Ferincz V⁹, Resch-Passini J⁵, Zimmermann-Ritterreiser M¹, Fritsch-Stork im Namen von BIOREG R¹⁰

¹Siemens Healthineers, Erlangen, Germany; ²Rheumatologische Schwerpunktpraxis, Hollabrunn, Austria; ³Landesklinikum Stockerau, Stockerau, Austria; ⁴Rheumatologische Praxis, Linz, Austria;

⁵Rheuma-Zentrum Wien-Oberlaa, Wien, Austria; ⁶Rheumatologische Schwerpunktpraxis, Wels, Austria; ⁷Universitätsklinik Innsbruck, Innsbruck, Austria; ⁸Rheumatologische Schwerpunktpraxis, Amstetten, Austria; ⁹Universitätsklinikum St. Pölten, St. Pölten, Austria; ¹⁰Gesundheitszentrum Mariahilf der ÖGK, Wien, Austria

Introduction: Rheumatologists face the challenge of selecting the most effective drug from a variety of biologics taking into account several factors including laboratory values, patient history and demographic data. Machine learning models can help overcoming the complexity of this choice by providing both the probability of success and an explanation for this prediction at the individual patient level. For this purpose, we developed prediction models for 5 different biological drugs using machine learning methods based on patient data derived from the Austrian Biologics Registry (BioReg).

Abstracts

Methods: Data from 1397 patients with 2004 baseline visits and 22 variables with at least 100 treat to target (ttt)-courses per drug were used from the BioReg biologics registry. Starting from the first visit of the ttt-course, different machine learning algorithms were trained for all drugs to predict the risk of ineffectiveness for each biological drug within the first 26 weeks. 5-fold cross-validation and hyperparameter optimization methods were applied to generate the best models. Model quality was assessed using the area under the receiver operator characteristic (AUROC). Using the Explainable AI method SHAP (SHapley Additive exPlanations; <https://shap.readthedocs.io/en/latest/index.html>) an approach from the mathematical field of game theory, the risk-reducing and risk-increasing factors were extracted.

Results: The best models per drug achieved an AUROC-score of: Abatacept: 0.71 (95% CI, 0.65–0.77), Adalimumab: 0.69 (95% CI, 0.62–0.76), Certolizumab: 0.77 (95% CI, 0.67–0.86), Etanercept: 0.69 (95% CI, 0.53–0.85), Tocilizumab: 0.74 (95% CI, 0.69–0.79). The 10 most predicting factors per drug were (+: risk-increasing for high values, -: risk-decreasing for high values, 0: nearly neutral; or stated otherwise):

Abatacept: VAS_GH (+), negative rheumatoid factor (risk-decreasing), age (+), ESR (+), BMI (-), intravenous administration (+), previous aTNF-therapy (+), TJC (+), DAS28 (-), male gender (+).

Adalimumab: GC (+), CRP [-], VAS Ph (-), disease duration (-), HAQ (+), VAS_GH (+), age (0), ESR (0), SJC (-), negative rheumatoid factor (risk-increasing).

Certolizumab: dosage (-), previous aTNF-therapy (+), negative rheumatoid-factor (risk-increasing), GC (+), age (+), BMI (-), other DMARDs (+), VAS_GH (+), SJC (+), HAQ (+).

Etanercept: VAS_GH (+), VAS Ph (-), anti-CCP positive (-), MTX-Co-therapy (no cotherapy strongly increased the predicted risk, whereas MTX-cotherapy slightly decreased the risk), negative rheumatoid factor (risk-decreasing), GC (+), BMI (-), CRP (-), other-DMARDs- (+), male gender (-).

Tocilizumab: VAS Ph (+), SJC (+), VAS_GH (+), ESR (+), TJC (+), previous aTNF-therapy (+), intravenous administration (-), CRP (+), HAQ (+), BMI (-). Due to the low AUROC-score (0.63 (95% CI, 0.59–0.68)) Golimumab was excluded from further analysis with Explainable AI frameworks.

Conclusion: The results show that the ineffectiveness of some biological drugs can be predicted with promising accuracy, comparable to similar research in (pooled) aTNF therapy [1]. Interestingly, factors that decrease the risk of ineffectiveness for one biological drug are found to be risk-increasing for another, indicating highly complex interactions. Machine Learning can be of help in the decision-process by disentangling these relations.

References

1. Guan Y, Zhang H, Quang D, Wang Z, Parker SCJ, Pappas DA et al (2019) Machine Learning to Predict Anti-Tumor Necrosis Factor Drug Responses of Rheumatoid Arthritis Patients by Integrating Clinical and Genetic Markers. *Arthritis Rheumatol* 71(12):1987–1996

2.8

Abdominal aortic calcification in rheumatoid arthritis patients—Results from a large cross-sectional study

Pieringer H¹, Puchner R², Lang D³, Sautner J⁴, Blessberger H³, Hintenberger R³

¹Klinik Diakonissen, Linz, Austria; ²Ordination, Wels, Austria; ³Kepler Universitätsklinikum, Linz, Austria; ⁴Landesklinikum Stockerau-NÖ Kompetenzzentrum für Rheumatologie, Stockerau, Austria

Introduction: Abdominal aortic calcification (AAC) is an often overlooked, but common finding. Despite its predictive value for cardiovascular (CV) events it has received much less attention than the arteries in the coronary system or the carotid vessels. Little is known about AAC in RA patients. Our primary aim was to investigate the prevalence of AAC in RA patients in comparison to the general population.

Methods: We used the National Health and Nutrition Examination Survey (NHANES) data set, a large US cross-sectional study with a complex, multi-stage sampling design, which represents the non-institutionalized

civilian resident population in the US. The 2013–2014 data set included measurement of AAC as well as data regarding RA status and comorbidities. Participants aged >40 years underwent dual-energy X-ray absorptiometry, including assessment of AAC. The presence of any calcification was accepted as presence of AAC.

Results: RA was associated with a higher prevalence of several CV risk factors: the odds ratio (OR) for arterial hypertension (HTN) was 2.83 (95% CI 1.77–4.52; $p < 0.001$), for diabetes 2.11 (95% CI 1.39–3.20; $p = 0.001$) and for current smoking 1.69 (1.19–2.40; $p = 0.006$). In addition, RA patients had a higher OR for suffering from poverty (OR 2.08; 95% CI 1.35–3.19; $p = 0.002$). Levels of total cholesterol, LDL cholesterol and triglycerides were comparable between the two groups. Chronic kidney disease (CKD) was more prevalent in the RA group and there was also a higher risk of albuminuria in RA patients (OR 1.94; 95% CI 1.18–3.20; $p = 0.013$). In univariate analysis AAC tended to be more prevalent in RA patients (OR 1.64; 95% CI 0.97–2.77) with a borderline significance of $p = 0.06$. After adjustment for potential confounders there was no independent association between RA and AAC (OR 1.23; 95% CI 0.71–2.10; $p = 0.43$). HTN, age and smoking status remained significantly associated with AAC after adjustment.

Conclusion: While a number of traditional CV risk factors were more common in the RA group, RA itself was not independently associated with AAC. It appears, that many of these risk factors already explain the presence of AAC in RA patients, more or less as some sort of summary measure of detrimental influences on the CV system. Therefore, the presence of AAC is a valuable piece of information in daily clinical practice and should prompt CV risk management also in RA patients.

2.9

Effectiveness of remote care interventions: a systematic review informing the 2022 EULAR points to consider for remote care in rheumatic and musculoskeletal diseases

Marques A¹, Bosch P², de Thurah A³, Meissner Y⁴, Falzon L⁵, Mukhtyar C⁶, Johannes WJ B⁷, Dejaco C⁸, Stamm T⁹

¹Higher School of Nursing of Coimbra Health Sciences Research Unit Nursing, Coimbra, Portugal; ²Klinische Abteilung für Rheumatologie und Immunologie, Medizinische Universität Graz, Graz, Austria; ³Aarhus University Hospital, Arhus, Denmark; ⁴Epidemiology and Health Services Research, German Rheumatism Research Centre, Berlin, Germany; ⁵Northwell Health, New York, United States; ⁶Vasculitis Service, Rheumatology Department, Norfolk and Norwich University Hospitals NHS Foundation Trust, Norwich, United Kingdom; ⁷Rheumatology, University Medical Center Utrecht Department of Rheumatology and Clinical Immunology, Utrecht, Netherlands; ⁸Klinische Abteilung für Rheumatologie und Immunologie, Medizinische Universität Graz und Landesweiter Dienst für Rheumatologie, Krankenhaus Bruneck, Graz, Austria; ⁹Section for Outcomes Research, Medical University of Vienna, Vienna, Austria

Introduction: To perform a systematic literature review (SLR) on different outcomes of remote care compared with face-to-face (F2F) care, its implementation into clinical practice and to identify drivers and barriers in order to inform a task force formulating the EULAR Points to Consider for remote care in rheumatic and musculoskeletal diseases (RMDs).

Methods: A search strategy was developed and run in Medline (PubMed), Embase and Cochrane Library. Two reviewers independently performed standardised data extraction, synthesis and risk of bias (RoB) assessment.

Results: A total of 2240 references were identified. Forty-seven of them fulfilled the inclusion criteria. Remote monitoring ($n=35$) was most frequently studied, with telephone/video calls being the most common mode of delivery ($n=30$). Of the 34 studies investigating outcomes of remote care, the majority addressed efficacy and user perception; 34% and 21% of them, respectively, reported a superiority of remote care as compared with F2F care. Time and cost savings were reported as major benefits, technical aspects as major drawback in the 13 studies that investigated drivers and barriers of remote care. No study addressed remote care implementation. The main limitation of the studies identified was the heterogeneity

Table 1 2.8 Characteristics of the RA group and n-RA group			
	RA	n-RA	p
Age (years)	57.5 (55.8–59.2)	46.8 (46.0–47.7)	<0.001
Female (%)	64.2 (55.7–71.9)	51.3 (49.7–52.9)	0.01
AAC (%)	38.5 (25.6–53.2)	27.7 (24.6–31.0)	0.06
BMI (kg/m ²)	30.6 (29.5–31.7)	29.0 (28.6–29.4)	0.003
RRsyst (mmHg)	127.8 (125.3–130.4)	121.4 (120.7–122.1)	<0.001
RRdiast (mmHg)	69.6 (67.2–72.1)	69.7 (68.9–70.5)	0.94
TC (mg/dl)	190.4 (184.3–196.5)	189.2 (187.2–191.1)	0.69
LDL (mg/dl)	110.5 (103.4–117.5)	111.1 (109.1–113.0)	0.86
Triglycerides (mg/dl)	132.6 (105.2–160.0)	120.0 (112.7–127.2)	0.40
Smoker (%)			
Never	45.7 (40.0–51.5)	57.2 (54.3–60.0)	0.02
Former	25.5 (17.0–36.3)	23.5 (21.4–25.7)	
Present	28.8 (20.8–38.4)	19.3 (17.2–21.6)	
Diabetes (%)	18.2 (12.7–25.4)	9.5 (8.6–10.6)	0.001
HTN (%)	67.2 (55.4–77.1)	42.0 (40.2–43.8)	<0.001
CKD (%)	6.3 (3.6–10.9)	1.6 (1.3–2.1)	<0.001
Albuminuria (%)			
A1	82.1 (73.0–88.7)	89.9 (88.6–91.1)	0.01
A2	14.8 (8.9–23.6)	8.7 (7.7–9.9)	
A3	3.1 (1.4–6.6)	1.4 (1.1–1.8)	
Poverty-Index <1	25.8 (16.6–37.9)	14.4 (11.6–17.6)	0.002

Data are represented as proportions (categorial variables) or mean (quantitative variables) with 95 % CI
AAC abdominal aortic calcification, HTN arterial hypertension, BMI body mass index, CKD chronic kidney disease (defined as creatin ≥ 1.5 mg/dl), RR_{syst} systolic blood pressure, RR_{diast} diastolic blood pressure, TC total cholesterol, LDL low density lipoprotein cholesterol
Poverty Poverty was accepted to present if the „Ratio of family income to poverty“ is < 1 (according to NHANES)

Table 2|2.8 Multivariable logistic regression analysis for RA and presence of AAC

Exposure variable	OR	95 % CI	p value
RA	1.23	0.71–2.10	0.43
<i>Age category</i>			
40–49	1	–	Ref.
50 < 59	1.64	1.07–2.53	0.03
60 < 69	2.37	1.52–3.69	0.001
70–80	8.30	5.20–13.27	<0.001
<i>Smoking status</i>			
Never	1	–	Ref.
Former	1.56	1.17–2.07	0.005
Current	2.28	1.43–3.65	0.002
HTN	1.43	1.09–1.88	0.01
Diabetes	1.03	0.78–1.36	0.80
CKD	1.20	0.58–2.51	0.60
Albuminuria	0.99	0.71–1.38	0.94

AAC abdominal aortic calcification, HTN arterial hypertension, CKD chronic kidney disease (defined as creatinine ≥ 1.5 mg/dl), RA rheumatoid arthritis

ity of outcomes and methods, as well as a substantial RoB (50% of studies with high RoB).

Conclusion: Remote care leads to similar or better results compared with F2F treatment concerning efficacy, safety, adherence and user perception outcomes, with the limitation of heterogeneity and considerable RoB of the available studies.

2.10

Ultrasound based withdrawal of biologics in rheumatoid arthritis (RA-BioStop)

Dejaco C^{1,2}, Gessl P¹, Husic R², Deimel T², Lackner A², Supp G², Hermann J², Smolen P³, Stradner M², Aletaha D³, Schantzer G², Mandl P³

¹Südtiroler Sanitätsbetrieb, Bruneck, Italy; ²Medizinische Universität Graz, Graz, Austria; ³Medizinische Universität Wien, Wien, Austria

Introduction: Discontinuation of biological (b)DMARDs may be considered in rheumatoid arthritis (RA) patients in persistent clinical remission[1]. Some earlier studies reported that baseline ultrasound may predict successful tapering or withdrawal of bDMARDs, while others found that ultrasound had little additional value over clinical parameters alone [2, 3]. The majority of these studies, however, were limited by small sample size, inadequate remission criteria and variable tapering regimens. The objective of this study was to test the hypothesis whether ultrasound-verified subclinical inflammation might predict a relapse in RA patients in stringent clinical remission who discontinue bDMARDs.

Methods: Prospective, phase IV clinical trial including RA patients in persistent clinical remission according to the ACR/EULAR criteria treat-

Abstracts

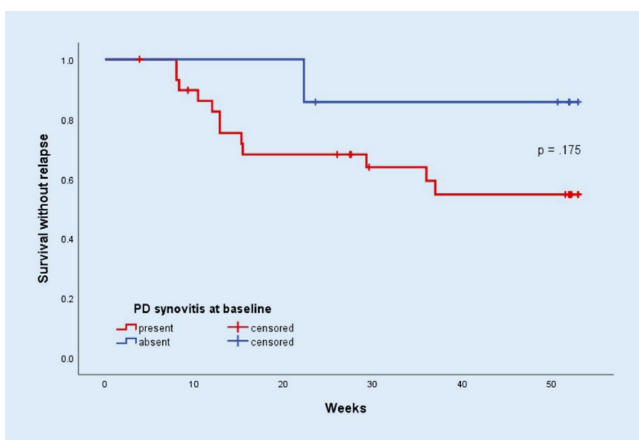


Fig. 1 | 2.10 ▲ Kaplan-Meier analysis of relapses according to presence or absence of Power Doppler (PD) synovitis at baseline

ed with a combination of conventional synthetic (cs)DMARD plus bDMARDs. Upon stopping the bDMARD, 9 study visits were conducted within 52 weeks. At each visit, patients underwent clinical examination and ultrasound of 14 joints. The primary hypothesis was that a Power Doppler (PD) score >0 predicted a relapse until week 16 after bDMARD cessation. Relapse was defined as change from remission to moderate/high disease activity according to the simplified disease activity index.

Results: Although 110 patients were required by the protocol, inclusion had to be stopped after reaching 38 (34.5%) due to insufficient recruitment. There were 9, 10 and 13 relapses between baseline and weeks 16, 24 and 52, respectively. Relapses till week 16 tended to be more common in patients with PD score >0 at baseline than in those without [9/30 (30.0%) vs. 0/7 (0%), $p=0.160$]. Similar observations were made for weeks 24 [9/30 (30.0%) vs. 1/7 (14.3%), $p=0.647$] and 52 [12/30 (40.0%) vs. 1/7 (14.3%), $p=0.383$]. Kaplan-Meier plot indicates the relapse-free survival in patients with and without PD+ synovitis at baseline (Fig. 1). PD scores were higher at the time of relapse as compared to the preceding visits [mean difference in the PD score 3.2 (± 4.5) points, $p=0.034$]. PD scores were also higher at visits preceding a relapse [mean 5.6 (± 3.9), $n=13$] as compared to the mean PD score across all visits of patients without a relapse [mean 2.0 (± 1.5), $n=24$, $p=0.003$, respectively]. There were trends towards a higher mean baseline PD score in patients who had a relapse between baseline and week 16 as compared to those who remained in remission (5.2 ± 5.8 vs. 2.3 ± 3.0 , $p=0.079$). Similar observations were made for relapses until weeks 24 and 52. No difference was observed comparing mean residual swollen or tender joint counts at baseline between patients with and without a relapse. There were 9 adverse events. All of them were mild to moderate.

Conclusion: In RA patients in strict clinical remission, PD assessment at baseline but not clinical joint count could help identify patients who will relapse

after the cessation of a bDMARD. Due to insufficient recruitment and limited power of the present trial, however, no definitive conclusion can be made.

References

- Smolen JS, Landewé RBM, Bijlsma JWJ et al (2020) EULAR recommendations for the management of rheumatoid arthritis with synthetic and biological disease-modifying antirheumatic drugs: 2019 update. Ann Rheum Dis Publ Online First. <https://doi.org/10.1136/annrheumdis-2019-216655>
- Naredo E, Valor L, De la Torre I et al (2015) Predictive value of Doppler ultrasound-detected synovitis in relation to failed tapering of biologic therapy in patients with rheumatoid arthritis. Rheumatol (oxford) 54:1408–1414. <https://doi.org/10.1093/rheumatology/kev006>
- Lamers-Karnebeek FB, Luime JJ, Cate DFT et al (2017) Limited value for ultrasongraphy in predicting flare in rheumatoid arthritis patients with low disease activity stopping TNF inhibitors. Rheumatol (oxford) 56:1560–1565. <https://doi.org/10.1093/rheumatology/kex184>

2.11

ACR/EULAR remission criteria for rheumatoid arthritis–2022 revision

Studenic P^{1,2}, Aletaha D¹, de Wit M³, Stamm TA¹, Alasti F¹, Lacaille D⁴, Smolen JS¹, Felson DT⁵

¹Medizinische Universität Wien, Wien, Austria; ²Karolinska Institutet, Stockholm, Sweden; ³EULAR PARE, Zaltbommel, Netherlands; ⁴University of British Columbia, Vancouver, Canada; ⁵Boston University School of Medicine, Boston, United States

Introduction: More than 10 years ago ACR and EULAR endorsed provisional criteria to define remission in RA, both Boolean and index-based. However, the agreement between these two sets of criteria was moderate, especially if patient global assessment (PGA) was >1 (0–10). Recent studies indicated that a higher threshold for the PGA improved this agreement. We aimed to provide evidence for ACR and EULAR by externally validating a revision of the Boolean remission criteria using a higher PGA threshold and to validate the provisionally endorsed index-based criteria.

Methods: Data from 4 randomised trials of biologic disease modifying antirheumatic drugs (bDMARDs) vs. methotrexate (MTX) or placebo were utilised. We tested a higher proposed PGA (Visual Analogue Scale; 0–10) threshold of 2 (Boolean 2.0) vs. the original threshold of 1 (Boolean 1.0). We analysed agreement between the Boolean and index-based criteria (SDAI, CDAI). We further examined how fulfilling each remission definition at 6 months predicted good physical function (HAQ ≤0.5) and radiographic non-progression (predictive validity) at one year. The validity of a Boolean definition omitting the PGA (BooleanX) was also assessed.

Results: Data from 2048 trial participants, 1101 with early (disease duration ≤2 years) and 947 with established RA were included. The proportion of participants in remission at 6 months increased when using Boolean2.0 compared to Boolean1.0 from 14.8–20.6% in early RA and 4.2–6.0% in established RA (Fig. 1). Agreement between Boolean2.0 and the SDAI or CDAI remission criteria was better than for Boolean1.0, particularly in

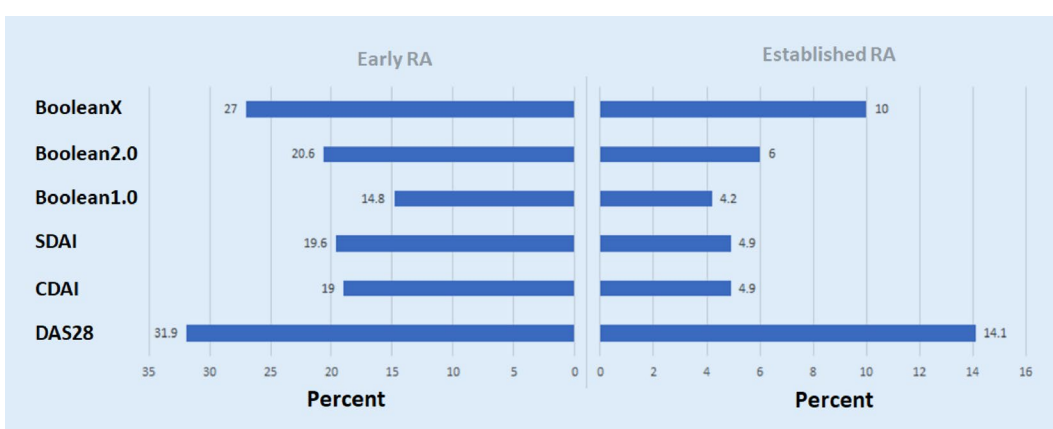


Fig. 1 | 2.11 ▲ Rates of remission by modified Boolean classifications, using a PGA threshold of 1.0 („Boolean“), 2.0 or omitting the PGA completely (BooleanX) as well as for the SDAI, CDAI and DAS28 definition. Rates at 6 months in % of total, separately depicted for early RA patients on the left and for established RA on the right

--

Table 1 | 2.11 Agreement Rates (% concordantly classified) between different modified Boolean remission definitions with the index-based remission definitions. Provided for 6 months

		6 months		
		Boolean1.0	Boolean2.0	BooleanX
SDAI	Early RA Overall % concordantly classified	93.4	95.9	90.8
	Established RA Overall % concordantly classified	98	98.2	94.6
CDAI	Early RA Overall % concordantly classified	93.2	94.6	89.1
	Established RA Overall % concordantly classified	97.7	97.1	93.3

Upper table: Agreement with SDAI remission, lower table with CDAI remission

early disease (Table 1). Boolean2.0, SDAI and CDAI remission criteria had similar positive likelihood (LR+) ratios to predict radiographic non-progression and a HAQ of ≤ 0.5 (Table 2). The proportion of participants achieving both good radiographic and functional outcomes, were similar for all remission definitions, from 57–60% (Boolean 1.0, 2.0, SDAI and CDAI: 58.6%, 57.3%, 59.2% and 60.4%), except for BooleanX (50.8%).

Conclusion: Using the Boolean2.0 definition increases the agreement with index-based remission criteria with the addition of classifying more patients in remission. Boolean2.0 SDAI and CDAI remission definitions perform equally and coincide with a good predictive value for both radiographic and functional outcomes. On this basis, these definitions were fully endorsed by ACR and EULAR.

2.12

Scoring structural damage in rheumatoid arthritis by ultrasound: results from a Delphi process and web-reliability exercise by the OMERACT US working group

Mandl P¹, Gessl I¹, Filippou G², Sirotti S², Terslev L³, Pineda C⁴, Keen H⁵, Backhaus M⁶, Bong D⁷, Cipolletta E⁸, Collado P⁹, Dejaco C¹⁰, Delle Sedie A¹¹, Duftner C¹², Berner Hammer H¹³, Iagnocco A¹⁴, Karim Z¹⁵, Möller I⁷, Naredo E¹⁶, Schmidt W¹⁷, Szkudlarek M¹⁸, Tamborrini G¹⁹, Wong P²⁰, Filippucci E⁸, Balint PV²¹, D'Agostino M²²

¹Klinische Abteilung für Rheumatologie, MUW, Wien, Austria;

²Rheumatology Department, Luigi Sacco University Hospital¹⁰ Milan, Italy;

³Center for Rheumatology and Spine Diseases, Copenhagen University Hospital Glostrup, Copenhagen, Denmark; ⁴Instituto Nacional de Rehabilitación, Mexico City, Mexico; ⁵School of Medicine and Pharmacology Fiona Stanley Hospital Unit, University of Western Australia, Perth, Australia;

⁶Department of Internal Medicine, Rheumatology and Clinical Immunology, Park-Klinik Weissensee Academic Hospital of the Charité, Berlin, Germany;

⁷Department of Rheumatology, Instituto Poal de Reumatología, Barcelona, Spain; ⁸Clinica Reumatologica, Università Politecnica delle Marche, Jesi, Italy; ⁹Hospital Universitario Severo Ochoa, Madrid, Spain; ¹⁰Hospital of Brunico (SABES-ASDAA), Department of Rheumatology, Brunico, Italy; ¹¹Rheumatology Unit, University of Pisa, Pisa, Italy; ¹²Department of Internal Medicine, Clinical Division of Internal Medicine II, Medical University of Innsbruck, Innsbruck, Austria; ¹³Department of Rheumatology, Diakonhjemmet Hospital, Oslo, Norway; ¹⁴Academic Rheumatology Centre, Department of Clinical and Biological Science, University of Turin, Turin, Italy; ¹⁵Department of Rheumatology, Mid Yorkshire NHS Trust, Yorkshire, United Kingdom; ¹⁶Department of Rheumatology, Hospital General Universitario Gregorio Marañón and Complutense University, Madrid, Spain;

¹⁷Immanuel Krankenhaus Berlin, Medical Centre for Rheumatology, Berlin-Buch, Germany; ¹⁸Department of Rheumatology, Copenhagen University Hospital at Køge, Copenhagen, Denmark; ¹⁹Ultrasound Center and Institute for Rheumatology¹⁰ Basel, Switzerland; ²⁰Division of Rheumatology, Department of Medicine and Therapeutics, The Chinese University of Hong Kong, Hong Kong, Hong Kong; ²¹3rd. Department of Rheumatology, National Institute of Rheumatology and Physiotherapy, Budapest, Hungary;

²²Rheumatology Unit, Università Cattolica del Sacro Cuore, Fondazione Policlinico Universitario Agostino Gemelli IRCCS, Rome, Italy

Introduction: Structural damage in rheumatoid arthritis (RA) includes bone erosions, cartilage change, and joint malalignment, which were historically evaluated on conventional radiography. Ultrasound (US) has been

Table 2 | 2.11 Percent of patients with a HAQ ≤ 0.5 , no increase in modified total Sharp Score (mTSS)/no radiographic progression, or both combined among those either fulfilling, or not fulfilling, the respective remission definition (Boolean1.0, Boolean2.0, BooleanX, SDAI-based, CDAI based definitions). Positive Likelihood ratios (LR+) for reaching the respective outcome at 12 months if remission is achieved at 6 months

Criteria fulfilled	HAQ ≤ 0.5 at 12 months			No increase in mTSS			Combined		
	No	Yes	LR+	No	Yes	LR+	No	Yes	LR+
<i>Early RA</i>									
Boolean1.0	43.3	85.9	6.19 (4.0–9.5)	65.6	78.5	1.76 (1.2–2.5)	31.7	67.5	3.54 (2.6–4.8)
Boolean2.0	41.5	80.6	4.23 (3.1–5.7)	64.4	79.3	1.85 (1.4–2.4)	29.6	65.2	3.19 (2.5–4.1)
BooleanX	40.5	74.1	2.76 (2.3–3.3)	63.1	79.5	1.86 (1.4–2.4)	28.4	60.3	2.59 (2.1–3.2)
SDAI	41.4	83.3	3.88 (3.1–4.9)	64.6	79.2	1.83 (1.2–2.5)	29.7	66.7	3.41 (2.6–4.4)
CDAI	41.6	83.7	4.25 (3.4–5.4)	64.8	78.9	1.81 (1.3–2.5)	29.9	67	3.46 (2.7–4.5)
<i>Established RA</i>									
Boolean1.0	29.2	72.5	5.86 (3.0–11.6)	32.6	37.5	1.23 (0.7–2.3)	12.1	22.5	2.02 (1.0–4.1)
Boolean2.0	28.7	68.4	4.19 (2.5–7.0)	32.4	40.4	1.38 (0.8–2.3)	11.8	24.6	2.27 (1.3–4.0)
BooleanX	28.1	57.9	2.42 (1.6–3.8)	31.3	46.3	1.76 (1.2–2.6)	11.6	21.1	1.86 (1.2–2.9)
SDAI	29	71.7	4.84 (2.7–8.5)	32.6	37	1.2 (0.7–2.1)	12	23.9	2.19 (1.1–4.2)
CDAI	28.7	76.1	4.84 (2.7–8.5)	32.6	37	1.2 (0.7–2.1)	11.8	28.3	2.74 (1.5–5.1)

Abstracts

shown to be a valid tool for the evaluation of both cartilage change and bone erosions in RA. We aimed to formulate definitions including semi-quantitative scoring systems for assessing structural damage on US and to test the reliability of such systems in a web-based exercise.

Methods: A Delphi survey was prepared by an OMERACT US Working Group (USWG) task force based on a previously published systematic literature review [1] and circulated between members of the group, including statements on normal US appearance of joint components, scanning technique and new definitions and scoring systems for bone erosion and joint malalignment. After agreement was achieved (>75% of grades 4–5 on 1–5 Likert scale) on the statements, still images of metacarpophalangeal and interphalangeal joints 2–5 in RA patients and healthy controls were acquired by taskforce members of the. A dataset of 100 anonymized images, representing various grades of the 3 aspects of structural damage: bone erosions, cartilage change and joint malalignment were created and utilized in two rounds of a web-based exercise. Intra- and inter-reader reliability of the two new scoring systems as well as that of a recently published US scoring system for cartilage by the USWG [2] was measured by kappa.

Results: Four Delphi rounds featuring 19 members were needed in order to reach agreement on a total of 9 statements. 4/12 statements were approved in the first, 2/6 in the second, 1/5 in the third and 2/2 in the fourth round. The final scoring systems and representative images are shown in □ Fig. 1. Twenty-two members participated in the web-based reliability exercise. The intra-reader reliability was almost perfect for bone erosion (kappa: 0.87) and cartilage change (kappa: 0.83) and substantial for malalignment (kappa of 0.72). The inter-reader reliability was almost perfect for bone erosion (kappa: 0.85), and substantial for cartilage change (kappa: 0.79) and malalignment (0.62).

Conclusion: In this first attempt to create a sonographic scoring system encompassing all aspects of structural damage, we demonstrate that US is a reliable tool for evaluating bone erosions, cartilage change and malalignment in the hand joints of patients with RA.

References

1. Gessl I et al (2021) Semin Arthritis Rheum 51(3):627–639
2. Mandl P et al (2019) Oct. Rheumatol (oxford) 58(10):1802–1811

2.13

Tenderness and radiographic progression in rheumatoid arthritis and psoriatic arthritis

Gessl I¹, Hana C¹, Deimel T¹, Durechova M¹, Hucke M², Konzett V¹, Popescu M³, Studenic P^{1,4}, Supp G¹, Zauner M¹, Smolen JS¹, Aletaha D¹, Mandl P¹

¹Klinische Abteilung für Rheumatologie, MUW, Wien, Austria; ²Abteilung für Innere Medizin und Gastroenterologie, Hepatologie, Endokrinologie,

Rheumatologie und Nephrologie, Klagenfurt, Austria; ³Department of Rheumatology, Hôpital Maisonneuve-Rosemont, Montreal, Canada;

⁴Department of Medicine (Solna), Division of Rheumatology, Karolinska Institute, Stockholm, Sweden

Introduction: In inflammatory arthritis swelling is regarded as a sign of synovitis and is associated with radiographic progression. The aim of this study was to assess the predictive value of tenderness in the absence of swelling with consideration of other potential risk factors for subsequent radiographic progression in rheumatoid arthritis (RA) and psoriatic arthritis (PsA).

Methods: Clinical and sonographic (greyscale and power Doppler (PD)) examination of 22 joints of the hand were performed in patients with RA and PsA. The impact of tenderness on progression after 2 years was analyzed in non-swollen joints for RA and PsA separately with multilevel mixed logistic regression calculating 3 models adjusting for age, sex, disease duration, PD, baseline erosion and joint space narrowing (JSN), swollen joint count and seropositivity.

Results: We included 1063 joints in 55 RA patients and 352 joints in 18 PsA patients. In RA, tenderness was associated with radiographic progression even after adjustment (OR 1.85 (95%CI 1.01–3.27), $p=0.047$), although the association of PD (OR 2.92 (95%CI 1.71–5.00), $p<0.001$) and erosions (OR 4.74 (95%CI 2.44–9.23), $p<0.001$) with subsequent structural damage was stronger. In PsA, we found a numerically positive association between tenderness and radiographic progression (OR 1.72 (95%CI 0.71–4.17), $p=0.23$). In contrast, similarly to RA, erosions (OR 4.62 (95%CI 1.29–16.54), $p=0.019$) and PD (OR 3.30 (95%CI 1.13–9.53), $p=0.029$) had a marked effect on subsequent structural damage.

Conclusion: Our findings imply that—in contrast to PsA—tenderness in RA is associated with subsequent radiographic damage. In both diseases, ad-

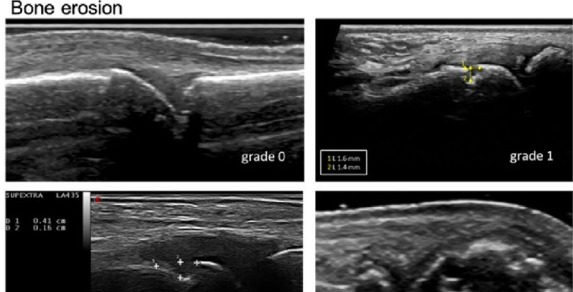
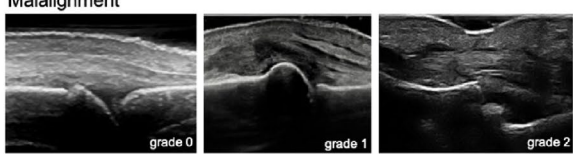
		Agreement	
Bone erosion	A 4-grade semiquantitative scoring system can be used to score erosions as follows: grade 0: intact cortical bone; grade 1: single small erosion (diameter: ≤2mm); grade 2: single large erosion (diameter: >2mm) or 2 small erosions; grade 3: 2 large erosions or >3 erosions, regardless of size. Both longitudinal and transverse scans should be considered, and the largest measure chosen for each erosion.	100%	
Cartilage change	A 3-grade semiquantitative scoring system (i.e. grade 0: normal cartilage; grade 1: minimal change: focal thinning or incomplete loss of cartilage; grade 2: severe change: diffuse thinning or complete loss of cartilage) can be used to grade hyaline cartilage change in RA.	80%	
Malalignment	A 3-grade semiquantitative scoring system can be used to grade malalignment as follows: 0: normal alignment; 1: subluxation or partial dislocation, where the two bone endings are malaligned so that one bone ending is dislocated from its normal position, but still within the articulation; 2: luxation or total dislocation, where the luxated bone ending moves beyond the articulation and the opposing bone ending. Bone position may be compared with a contralateral or similar intact joint if available.	94%	

Fig. 1 | 2.12 ▲ Final definitions of scoring systems and representative images of the scoring systems for bone erosion (a), cartilage change (b) and malalignment (c)

ditional risk factors, such as sonographic signs for synovitis and baseline radiographic damage are associated with radiographic progression.

3 Kinderrheumatologie

3.1

Long-term data of children with chronic non-bacterial osteomyelitis (CNO)-Indicators for remission, disease activity and severe disease

Reiser C^{1,2}, Klotsche J^{3,4}, Hospach T⁵, Windschall D^{6,7}, Heubner G⁸, Trauzeddel R⁹, Grösch N¹⁰, Niewerth M¹⁰, Minden K^{3,4}, Girschick H^{11,12}

¹Pädiatrie, Landeskrankenhaus Bregenz, Bregenz, Austria; ²University Children's Hospital Tuebingen, Tübingen, Germany; ³Deutsches Rheuma-Forschungszentrum Berlin, ein Institut der Leibniz-Gemeinschaft Berlin, Germany; ⁴Charité–Universitätsmedizin Berlin, corporate member of Freie Universität Berlin, Humboldt Universität zu Berlin, and Berlin Institute of Health, Berlin, Germany; ⁵Department of Pediatrics, Olgahospital, Klinikum Stuttgart, Stuttgart, Germany; ⁶St.-Josef-Stift, Sendenhorst, Germany; ⁷University of Halle-Wittenberg, Halle, Clinic for Pediatric and adolescent Rheumatology, Halle, Germany; ⁸Städtisches Klinikum Dresden-Neustadt, Klinik für Kinder- und Jugendmedizin, Dresden, Germany; ⁹Fachambulanz Kinderrheumatologie, Helios Klinikum Berlin-Buch, Klinik für Kinder- und Jugendmedizin, Berlin, Germany; ¹⁰Deutsches Rheuma-Forschungszentrum Berlin, ein Institut der Leibniz-Gemeinschaft, Berlin, Germany; ¹¹Vivantes Klinikum Friedrichshain, Children's Hospital, Berlin, Germany; ¹²Childrens' Hospital, University of Wuerzburg, Würzburg, Germany

Introduction: To document the long-term course of CNO, to assess risk factors for severe disease course and to define remission criteria.

Methods: From 2015–2020 all patients with a confirmed diagnosis of CNO, who were registered in the NPRD during their first year of disease course and at least one follow-up visit, were included in this analysis.

Results: Additionally to the previously reported cross-sectional analysis of almost 800 CNO patients, a data set of 314 eligible patients including up to 5 years of follow-up visits was analysed. Selected patients' characteristics are described. The analysis of the location of the lesions showed that the distribution changed over the years. Whereas in the first year of disease course sites like vertebrae or mandibula were inflamed (8% and 2% of all affected sites), these sites completely resolved over time, while other sites like pelvis or tibia (18%/20%) remained affected after 5 years. Initially, patients were mainly treated with non-steroidal anti-rheumatic drugs (NSAIDs). Inflammation of pelvis or femur at baseline posed an elevated risk for long term severe disease (OR 1.51/1.61, each $p=0.0001$). Other risk factors for severe disease were raising numbers of lesions, elevated ESR (erythrocyte sedimentation rate) and multifocal disease (defined as more than one lesion) in the beginning. The risk for arthritis increased with the initially higher number of lesions. Items defining remission best were PRDA <1, patient reported pain score and number of inflammatory bone lesions. The composite Childhood health assessment score (C-HAQ) and patient reported overall well-being did not correlate with inactive disease.

Conclusion: The NPRD long-term cohort documents a large number of children and adolescents with CNO. Most of the patients were treated effectively with non-steroidal anti-inflammatory drugs, second-line treatment in a limited number of patients are disease-modifying agents, steroids or bisphosphonates. An improvement of patient-, physician- and imaging-defined disease activity measures was documented, suggesting CNO generally as benign disease with a modest number of complicated disease course. Remission defining items and risk factors for severe disease course were defined.

3.2

Osteoidosteom, auch bei Hüftschmerzen eine wichtige Differentialdiagnose – ein Fallbericht

Sailer-Höck M¹, Eberle G², Putzer D², Schweigmann G²

¹Department für Kinder- und Jugendheilkunde, Innsbruck, Österreich;

²Universitätsklinik für Radiologie, Innsbruck, Österreich

Einleitung: Im Dezember 2019 wurde uns eine 13 Jahre alte Patientin mit Verdacht auf eine rheumatische Erkrankung zugewiesen.

Methoden: Das Mädchen klagte seit 9 Monaten über Schmerzen in der rechten Hüfte. Diese traten anfänglich nach sportlicher Aktivität auf, später auch nachts. Es wurde zunächst die Diagnose Coxalgie rechts mit Muskelansatztendinitis des Musculus Abductor longus gestellt. Einige Monate später wurde mittels Magnetresonanztomografie eine Partialruptur im Ansatzbereich der Ilioopsassehne diagnostiziert. Physiotherapie und die kurzfristige Einnahme von Ibuprofen und Paracetamol brachten kaum Besserung. Im November 2019 wurde neuerlich eine MRT Untersuchung durchgeführt und die Patientin zu uns überwiesen.

Resultate: Bei der Untersuchung zeigten sich bei Beugung des rechten Hüftgelenks Schmerzen an der Innenseite des Oberschenkels proximal. Hier war auch ein deutlicher Druckschmerz und ein Muskelhartspann. Weiters bestand eine deutliche Muskelatrophie des Musculus Gluteus rechts und der Oberschenkelmuskulatur rechts. Laborbefunde waren alle unauffällig. In den von der Patientin mitgebrachten MRT-Bildern zeigte sich das typische Bild eines Osteoidosteoms. Es wurde eine CT-gezielte Radiofrequenzablation durchgeführt. Danach wurde die Patientin rasch beschwerdefrei.

Schlussfolgerungen: Das Osteoidosteom ist ein benigner, Knochen bildender Tumor geringer Größe, der von den Osteoblasten ausgeht und vor allem in der Corticalis der langen Röhrenknochen auftritt. Das Erkrankungsalter liegt meist zwischen dem elften und zwanzigsten Lebensjahr. Histologisch typisch ist eine nidusartige Struktur mit einem zellreichen, stark vaskularisierten Gewebe, umgeben von einer oft ausgedehnten Knochennekrose. Die typischen, meist nächtlichen Schmerzen sind durch die Prostaglandinproduktion der Tumorzellen bedingt. Nichtsteroidale Antirheumatika wirken meist schmerzlindernd. Ein Osteoidosteom kann spontan ausheilen. Die Therapie ist eine CT-gesteuerte Frequenzablation des Tumors. Die Diagnose eines Osteoidosteoms kann schwierig sein, da bei gelenknaher Lage eine reaktive Synovitis den diagnostischen Nidus klinisch und auch radiologisch maskieren kann.

4 Rehabilitation

4.1

Rehabilitation bei SLE

Stummvoll G¹, Mur E², Wiederer C³

¹SVS, Wien, Österreich; ²Medizinische Universität Innsbruck, Innsbruck, Österreich; ³Klinikum Am Kurpark, Baden, Österreich

Einleitung: Obwohl Bewegung und Training (in Ergänzung zu Medikation) bei vielen rheumatischen Erkrankungen allgemein empfohlen werden, finden spezifische nicht-pharmakologische Therapieformen bei Patienten mit systemischem Lupus erythematoses (SLE) oft wenig Berücksichtigung bei der Erstellung des individuellen Behandlungsplans. Die EULAR hat in ihren Empfehlungen zur Behandlung des SLE im Jahr 2008 physische Aktivität, Gewichtskontrolle, Nikotinabusus als positive Lebensstilmodifikationen – speziell für Patienten mit erhöhtem kardiovaskulären Risiko – empfohlen, wobei die Evidenzlage diesbezüglich nach wie vor überschaubar ist. Es wird nachfolgend der Versuch unternommen, die bestehende Evidenz für nicht-pharmakologische Therapieformen bei SLE aufzuzeigen und mit einer Expertenmeinung aus österreichischer Sicht zu verbinden.

Methoden: Suche in der PubMed mit den Schlagworten „lupus erythematosus“ AND „exercise OR rehabilitation“ ((„lupus vulgaris“[MeSH Terms] OR („lupus“[All Fields] AND „vulgaris“[All Fields])) OR „lupus vulgaris“[All

Abstracts

Box 1 | 4.1 Beispiel eines individuellen Behandlungsplans bei SLE

Patientin NN, Beispiel für einen individualisierten Behandlungsplan bei SLE

Anamnese: SLE, Migräne, Lumbalgien/Cervikalgien, Schmerzen li Schulter; berufstätig

Ärztliche Visiten/Untersuchungen: Aufnahmeuntersuchung, 1. Visite, Fachärztliche Visite, Visite, Zwischenuntersuchung (1x), Enduntersuchung. Weitere Visiten/Untersuchungen: Aufnahmeuntersuchung (Therapie), Ernährungsvisite (1x), Psychologisches Einzelgespräch (2x), Berufsberatung (1x).

Vorträge: Vortrag „Schmerzen verstehen“, Vortrag „Work-Life-Balance“, Vortrag „Hygiene Covid 19“, Vortrag „Rheuma verstehen“, Vortrag „Rücken und Wirbelsäule“.

Therapie: Bewegungstherapie, einzeln, trocken (6x), Wirbelsäulengruppe trocken Basis (8x) Gruppe UE Wasser Basis (9x), Schultergruppe im Wasser Basis (5x), Trainingstherapie Fahrrad 1 (7x), Trainingstherapie Seilzug (2x), Haltung aktiv 1 (1x), Haltung aktiv 2 (1x), Haltung aktiv 3 (1x), Haltung aktiv 4 (1x), Massage (5x), Massage auf dem Wasserbett (1x), Paraffinpackung (5x), Fango (2x), Schwefelbad (4x), Stereodynator (Elektrotherapie) (6x), Ultraschall (6x), Beckenbodentraining (2x).

Fields] OR „lupus“[All Fields] OR „lupus erythematosus, systemic“[MeSH Terms] OR „lupus“[All Fields] AND „erythematosus“[All Fields] AND „systemic“[All Fields]) OR „systemic lupus erythematosus“[All Fields] AND erythematosus[All Fields]) AND ((„exercise“[MeSH Terms] OR „exercise“[All Fields]) OR („rehabilitation“[Subheading] OR „rehabilitation“[All Fields] OR „rehabilitation“[MeSH Terms])). Danach weitere Eingrenzung auf Arbeiten mit klinischen Daten zu Bewegungstherapie bzw. Rehabilitationsmaßnahmen bei SLE. Abstimmung der systematischen Suchergebnisse unter den Autoren, die über langjährige klinische Erfahrung in der medikamentösen und nicht-pharmakologischen Therapie des SLE verfügen – im Sinne einer „internen Evidenz“.

Resultate: Nachdem sich bei der systematischen Suche in der PubMed am 01.09.2022 mit den Schlagworten „lupus erythematosus“ AND „(exercise OR rehabilitation)“ 1136 Ergebnisse fanden, wurde die Suche auf die letzten 10 Jahre, auf Studien am Menschen und auf systematische Reviews/Metanalysen in deutscher oder englischer Sprache eingeschränkt (36 hits). Diese Arbeiten wurden hinsichtlich der Einschlusskriterien beurteilt und analysiert (10 Arbeiten). Die 3 umfassendsten Arbeiten zur Thematik sind im Literaturverzeichnis angeführt. Entsprechend der aktuellen Literatur besteht Evidenz für die Nützlichkeit von aerober Trainingstherapie bei Fatigue und bei Depressio. Bewegungstherapie verbesserte die Lebensqualität im SF-36. Kognitive Therapien wirken sich positiv auf die Lebensqualität und die Schmerzen von Seiten der Grunderkrankung aus.

Schlussfolgerungen: Expertenmeinung. Gerade eine sehr heterogene Erkrankung wie der SLE muss mit einem stark individuell konzipierten und auch allfällige Nebendiagnosen berücksichtigenden Therapieplan versehen werden. Das multimodale Konzept eines Rehabilitationszentrums mit einem breiten Spektrum von Therapieoptionen kommt SLE-Patienten dabei sehr entgegen, da es die Möglichkeit bietet, aktive Bewegungstherapie im Wasser, im Turnsaal und im Freien auszuüben, ergänzt um zahlreiche „passive“ Therapieformen (Elektrotherapie, Wärmetherapie, Massage). Zusätzlich eröffnen sich im Rahmen der Rehabilitation Möglichkeiten zu Lebensstilmodifikationen (u. a. auch durch diätologische und psychologische Beratung), Raucherentwöhnung sowie zur Berufsberatung – wie aus dem exemplarischen Behandlungsplan in Box 1 ersichtlich. Aus der Literatur und der Erfahrung kann somit abgeleitet werden, dass SLE-Patienten jeden Alters und jeder Krankheitsdauer von einem individualisierten Rehabilitationsprogramm profitieren können und ihnen bei entsprechender Indikation die Möglichkeiten eines stationären oder ambulanten Rehabilitations-Verfahrens eröffnet werden sollten.

Literatur

- Chang A et al (2021) Systematic review of digital and non-digital non-pharmacological interventions that target quality of life and psychological outcomes in adults with Systemic Lupus Erythematosus. *Lupus* 30(7):1058–1077
- O'Dwyer T et al (2017) Exercise and physical activity in systemic lupus erythematosus: A systematic review with meta-analyses. *Semin Arthritis Rheum* 47:204–215
- Monthida Fangham et al (2019) Non-Pharmacologic Therapies for Systemic Lupus Erythematosus. *Lupus* 28(6):703–712

5 Sonstiges

5.1

Engraftment of NSG-DR4 mice with human mononuclear cells of rheumatoid arthritis patients induces arthritis

Rupp J¹, Fessler J², Hayer S³, Dreo B¹, Lackner A¹, Fasching P⁴, Helmberg W⁵, Schlenke P⁵, Thiel J¹, Steiner G³, Weyand CM⁶, Stradner MH¹

¹Medical University of Graz, Division of Reumatology and Immunology, Graz, Austria; ²Medical University of Graz, Division of Immunology and Pathophysiology, Graz, Austria; ³Medical University of Vienna, Division of Rheumatology, Vienna, Austria; ⁴Steiermärkische Krankenanstaltengesellschaft m.b.H., Institut für Krankenhaushygiene und Mikrobiologie, Graz, Austria; ⁵Medical University of Graz, Department of Blood Group Serology and Transfusion Medicine, Graz, Austria; ⁶Mayo Clinic School of Medicine and Sciences, Division of Rheumatology, Department of Medicine, Rochester, MN, United States

Introduction: Emerging evidence supports an important role for T cells in the genesis of rheumatoid arthritis (RA). The pathogenesis of this incurable disease is still elusive. HLA class II genes however, such as HLA-DRB1*0401 (HLA-DR4), confer the strongest genetic risk and suggest involvement of CD4+ T cells. Existing mouse models mimic specific aspects of the disease but do not fully recapitulate the human immune system. Thereby current research is limited and would profit from a humanized mouse model. We aimed to identify arthritogenic cells by transferring HLA-DR4+ peripheral blood mononuclear cells (PBMC) of RA patients into NSG-DR4 mice. Thereby generating a novel mouse model with inflammatory joint disease, only triggered by the transfer of human immune cells

Methods: Humanized NSG-DR4 mice (NSG-AB0 Tg(HLA-DR4)) were generated by injecting PBMC of HLA-DR4 positive patients or controls. Engraftment within peripheral blood, bone marrow, skin, liver, and spleen was assessed comprehensively using multicolor flow cytometry. Development of RA was monitored by examination of the joints, followed by micro computed tomography analysis and histology. Joints were analyzed regarding pannus formation, bone erosions, cartilage damage, and human cell infiltration.

Results: Here, we show that DR4+ T cells of the peripheral blood of RA patients are capable of inducing an RA-like disease in NSG-DR4 mice. These mice recapitulate different hallmarks of the disease including immune cell infiltration, pannus formation, increased osteoclastogenesis, cartilage damage, and bone erosions. Compared to healthy controls, cells of RA patients are more likely to develop inflammatory joint disease in these mice (RA donor 70% vs. healthy control 20%, $p=0.00196$). T-helper 1 (Th1) cells, dominated the human immune cell composition in mice, while regulatory T cells (Tregs) were diminished compared to donor PBMC composition. Transfer of in vitro Th1 polarized T cells increased arthritis incidence.

Conclusion: Arthritogenic cells found in the peripheral blood of RA patients are capable of inducing an RA-like disease in NSG-DR4 mice. This novel mouse model will allow to identify these cells on a patient-personalized level.

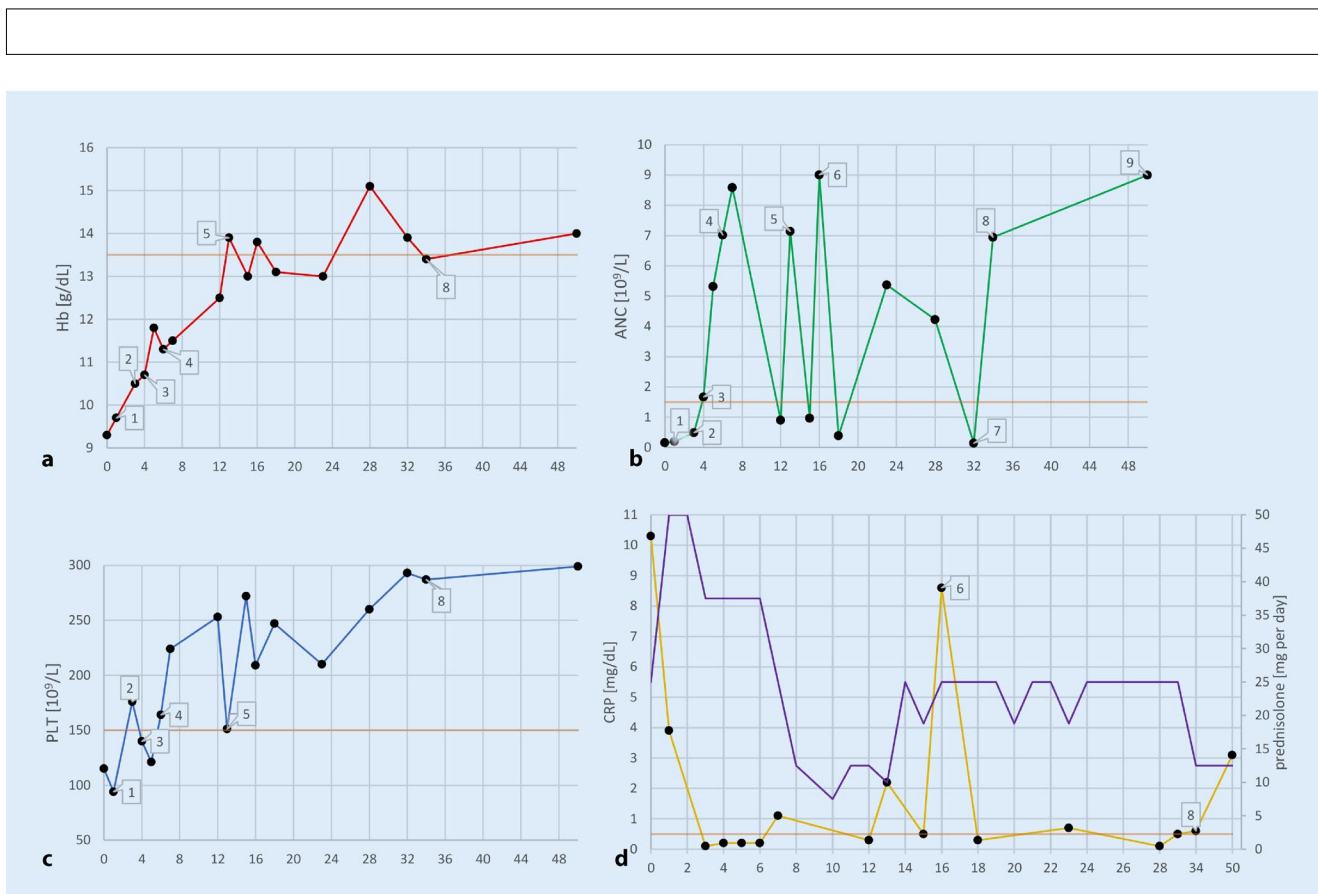


Abb. 1 | 5.1 ▲ a-d Hämoglobin-Gehalt (Hb), absolute Neutrophilenzahl (ANC), Thrombozyten (PLT) sowie C-reaktives Protein (CRP) im zeitlichen Verlauf (in Wochen, ab Beginn des ersten Krankenhausaufenthaltes). Der jeweilige untere Referenzwert für Hb, ANC, PLT bzw. der obere Referenzwert für CRP sind als orange horizontale Linien gekennzeichnet (Hb: 13.5 g/dL, ANC: 1.5 × 10⁹/L, PLT: 150 × 10⁹/L, CRP: 0.5 mg/dL). Abbildung D zeigt zusätzlich zum CRP-Verlauf die eingenommene Prednisolon-Dosis. Weiters sind folgende Ereignisse innerhalb der Diagramme gekennzeichnet: 1: Prednisolon-Steigerung auf 50 mg tgl. – nach 1 Woche; 2: Beginn mit Methotrexat p. o. (20 mg 1 × wöchentlich) – nach 3 Wochen; 3: 1. Gabe Rituximab 1000 mg – nach 4 Wochen; 4: 2. Gabe Rituximab 1000 mg – nach 6 Wochen; 5: Umstellung auf Methotrexat s. c. (25 mg 1 × wöchentlich) – nach 13 Wochen; 6: Fieberhafter Infekt mit CRP- und ANC-Anstieg – nach 16 Wochen; 7: ANC Abnahme aufgrund fehlender G-CSF Applikation bei Incompliance – nach 32 Wochen; 8: Beendigung von Methotrexat, Prednisolon-Reduktion auf 12.5 mg täglich, zweiter Zyklus Rituximab (1000 mg am Tag 1 sowie Tag 15) – nach 34 Wochen; 9: Ausdehnung des G-CSF Intervalls von einmal alle 5 Tage auf einmal wöchentlich – nach 50 Wochen



Abb. 2 | 5.1 ▲ Hautulzerationen femoral links (a) sowie gluteal rechts (b) zum Aufnahmezeitpunkt

5.2

Felty-Syndrom – Fallbericht aus der Rheuma-Ambulanz St.Pölten

Wegscheider C

2. Medizinische Abteilung, UK St.Pölten, St.Pölten, Österreich

Einleitung: Das Felty-Syndrom wurde im Jahr 1924 vom US-amerikanischen Arzt Augustus Roi Felty als eine Trias aus chronischer Arthritis, Splenomegalie und Leukopenie erstmals beschrieben. Auch fast 100 Jahre danach stellt dieses Krankheitsbild mitunter noch eine diagnostische und therapeutische Herausforderung dar. Dieser Fallbericht aus der Rheuma-Ambulanz St.Pölten veranschaulicht mögliche Probleme und gibt außerdem eine aktuelle Übersicht über einzelne Aspekte des Felty-Syndroms.

Methoden: Ein 42-jähriger Mann mit vorbekannter seropositiver rheumatoider Arthritis wurde zur Abklärung einer neu aufgetretenen Panzytopenie sowie multipler Hautulzerationen stationär aufgenommen. Zum Ausschluss einer malignen Ursache erfolgten eine Beckenkammbiopsie, eine Sonographie der Lymphknotenstationen sowie eine CT Thorax/Abdomen. Letztlich wurde die Diagnose eines Felty-Syndroms gestellt und eine Therapie mit Methotrexat in Woche 3 eingeleitet, welche kurz darauf (Woche 4) um Rituximab ergänzt wurde (1000 mg an Tag 1 und Tag 15). Begleitend erfolgte die Gabe von G-CSF und Prednisolon. Bei inadäquatem Ansprechen bzgl. Arthritis und Neutrophilenzahl war im Verlauf die Umstellung von Methotrexat auf Hydroxychloroquin geplant, welche aufgrund von Incompliance jedoch nicht möglich war. Die derzeitige Therapie besteht aus Rituximab, G-CSF und Prednisolon. Weitere Thera-

Abstracts

pieoptionen (Splenektomie, Versuch mit JAK-Inhibitor) werden aktuell diskutiert. Der Patient ist weiterhin in unserer Ambulanz angebunden zur regelmäßigen klinischen und laborchemischen Verlaufskontrolle. **Resultate:** Sowohl Anämie als auch Thrombopenie besserten sich bereits in den ersten Wochen (siehe □ Abb. 1), zur Aufrechterhaltung einer stabilen Neutrophilenzahl war aber bis Woche 7 eine zweitägliche G-CSF Gabe (Filgrastim 480 µg) notwendig. Auch die Prednisolon-Dosis konnte von initial 50 mg täglich nur langsam reduziert werden auf zuletzt 12,5 mg täglich in Woche 50. Die Hautulzerationen (siehe □ Abb. 2) heilten unter der immunsuppressiven Therapie vollständig ab. Die G-CSF Therapie wurde im betrachteten Zeitraum von 50 Wochen gut vertragen, derzeit erfolgt die Applikation einmal wöchentlich. In der initialen Beckenkammbiopsie war eine klonale T-Zellenpopulation nachweisbar, ohne jedoch die Kriterien einer T-LGL Leukämie zu erfüllen. Dbzgl. ist eine durchflusszytometrische Kontrolle im weiteren Verlauf geplant.

Schlussfolgerungen: Das Felty-Syndrom ist ein seltes und mitunter schwer behandelbares Krankheitsbild. Zwar hat sich die Prognose durch den Einsatz von Methotrexat, Rituximab und G-CSF in den letzten Jahrzehnten deutlich verbessert, allerdings bedarf es in Zukunft, wie durch diesen Fallbericht verdeutlicht, weiterer Therapieoptionen. JAK-Inhibitoren zeigten eine Verbesserung der Neutropenie bei Patienten mit rheumatoider Arthritis und T-LGL Leukämie. Da das Felty-Syndrom pathogenetische Gemeinsamkeiten mit der T-LGL Leukämie haben dürfte, könnten JAK-Inhibitoren eventuell auch in der Therapie des Felty-Syndroms nützlich werden.

5.3

Innovation in rheumatology teaching—The RheumEscape room

Reisch M¹, Kickinger D¹, Bosch P², Puchner R³, Dejaco C⁴

¹LK Lilienfeld, Lilienfeld, Austria; ²Meduni Graz, Graz, Austria; ³ÖGR, Wels, Austria; ⁴Krankenhaus Bruneck, Bruneck, Italy

Introduction: Over the years, methods in medical teaching have changed giving more emphasis on applied medicine, critical thinking and learner-centered activity. An Escape Room (ER) is a popular adventure game, where participants have to cooperate as a team to escape from a locked room by completing tasks and solving a series of puzzles. ERs can also be used in medical teaching as an entertaining way to acquire or refresh knowledge, to support critical thinking and team building as well as to improve communicative, technical and non-technical skills. We adapted this game design and created an ER in rheumatology with the objective to transfer a defined amount of knowledge in rheumatology to medical students and residents.

Methods: An educational ER in the field of rheumatology was developed and performed nine times with four to six medical students or residents per session. All groups had to complete the ER within 90 min including a briefing of 15 min. In the ER, the participants had to use their rheumatological knowledge, critical thinking and teamwork to unlock several puzzles on various rheumatological topics. The focus of the content was mainly on frequent diseases, common therapeutic problems and the implication of assessment tools. Afterwards, a didactic debriefing was done, giving a summary of all riddles and answering questions of the participants. To test the feasibility and effectiveness of this new teaching method, students and residents were asked to complete an anonymous feedback form with 15 questions. The answers of ten questions were rated on a 10-point Likert scale (0 = does not apply; 10 = totally applies). Furthermore, five questions were in a single ($n=4$) or multiple-choice format ($n=1$). Descriptive statistical were conducted to summarize the data.

Results: A total of 28 medical students and 19 residents completed the questionnaire. On a 10-point scale, the participants rated on average with 8.9 points [standard deviation 1.92; range 5–10] that they acquired new medical skills and with 8.9 points [1.78; 3–10] that they enhanced their knowledge in rheumatology. All medical students and residents had the feeling, that they could participate actively in this game-based learning method. On average, they responded with 9.9 points [0.15; 9–10] that the ER was entertaining and 9.7 points [0.97; 4–10] that teambuilding was

improved by the game. Furthermore, they gave a score of 9.7 points [0.15; 9–10] that they would recommend this learning method to a friend and a score of 9.9 points [0.41; 8–10] that they wanted to do a medical ER again.

Conclusion: A rheumatological ER is a unique complementary approach for medical education. It is a feasible and entertaining way of teaching, associated with a perceived increase in rheumatological knowledge, teambuilding and communication skills. Further studies assessing the level of competence before and after the ER are needed to ensure the learning success and to compare the rheumatological ER with other traditional teaching methods.

6 Fallstudien

6.1

Fallbericht einer Jugendlichen mit Takayasu Arteritis

Valent I¹, Ulbrich A¹, Zimpfer D², Kitzmüller E³, Hojreh A⁴, Emminger W¹

¹Medizinische Universität Wien, Universitätsklinik für Kinder- und Jugendheilkunde, Klin. Abteilung für Päd. Nephrologie und Gastroenterologie, Kinderrheumaambulanz, Wien, Österreich; ²Medizinische Universität Graz, Universitätsklinik für Chirurgie, Klinische Abteilung für Herzchirurgie, Herzzentrum Graz, Graz, Österreich; ³Medizinische Universität Wien, Universitätsklinik für Kinder- und Jugendheilkunde, Klinische Abteilung für Pädiatrische Kardiologie, Wien, Österreich; ⁴Medizinische Universität Wien, Universitätsklinik für Radiologie und Nuklearmedizin, Klinische Abteilung für Allgemeine Radiologie und Kinderradiologie, Wien, Österreich

Einleitung: Dieser Fallbericht handelt von einer 15-jährigen Patientin, bei welcher seit ca. 2 Monaten rez. verschwommenes Sehen, vermehrter Schwindel mit Kollapsneigung sowie Kopfschmerzen und Sensibilitätsstörungen an den Extremitäten bestanden. Die linke Körperhälfte sei seit Beginn der Beschwerden vermehrt blass, eingeschränkt beweglich und leicht schmerhaft, zusätzlich beständigen Hypästhesien, besonders bei Aktivität, ohne Kraftminderung. Im Jänner 2020 erfolgte bei fragl. Halbseitensymptomatik die Vorstellung beim Kinderkardiologen, welcher mittels US eine schwere, beinahe komplett Stenose der Halsarterien feststellte. Acetylsalicylat wurde begonnen und eine MR-Angio organisiert, hier zeigten sich folgende Pathologien: Der Tr. brachiocephalicus, die rechten Aa. subclav. und carotis com. waren nicht darstellbar. Im Abgangsbereich der li. A. subclavia (ASS) zeigte sich eine höhergradige 15 mm lange Stenose. Nach dieser Stenose geht die sehr kaliberstarke li. A. vertebralis (AVS) ab, die nicht stenosiert ist. Die re. A. vertebr. ist retrograd perfundiert bis Höhe C5, dann weiter proximal verschlossen. Somit ist die AVS das einzige hirnversorgende Gefäß. Aufgrund dieses Befundes erfolgte die stationäre Aufnahme bei V.a. Takayasu Arteritis. In den immunol. Befunden zeigten sich ANA 1:160 nukleolär, BSG 18/46 mm/h und ein Calprotectin von 15119 ng/ml. Es bestand eine deutliche RR-Differenz, mit normot. bzw. hypot. an den OE und hypert. Werten an den UE. Es wurde sogleich mit einem Cortisonstoß begonnen und anschließend mit Prednisolon 1 mg/kg/d fortgesetzt. Zwei Tage darauf wurde die immunsupp. Therapie um den IL-6 Rezeptorantagonisten Tocilizumab (400 mg i.v.) erweitert. In der Dopplersonographie der Halsgefäße zeigte sich ein Verschluss der großen oberen Gefäße konsistent mit den Befunden des MRTs. Es wurde zur weiteren Diagnostik ein PET/MRT sowie ein CT der supraaortalen Gefäße durchgeführt, in welchen sich kein Nachweis einer floriden Arteritis zeigte. In der CT bestätigte sich ein vollständiger Verschluss der A. carotis int. bds, eine ausgeprägte Kollateralenbildung über die Halsmuskulaturgefäße mit Kontrastierung der cran. Gefäße über die beiden Aa. vertebr. Die rechte, proximal verschlossene A. vertebr. wird hierbei auf Höhe HWK6 über Kollateralen versorgt. Die kaliberkräftiger AVS entspringt mit höchstergradiger kurzstreckiger Abgangstenose der ASS poststenotisch aus eben dieser. Somit ist die AVS das einzige hirnversorgende Gefäß. Ende Jänner erfolgte per Thorakotomie eine Anlage eines Goretex-Graft (6 mm) von der Aorta ascend. auf die ASS um eine adäquate Versorgung des Gehirns

zu gewährleisten, indem die langstreckige Stenose der ASS vor Abgang der AVS überbrückt wird. Postoperativ wurde niedrig dosiert Acetylsalicylat re-establiert und mit einem ADP-Rezeptorantagonisten ergänzt, die immunsupp. Therapie mit Tocilizumab wurde nach 3 i.v.-Gaben auf s.c. (162 mg zuerst wöchentlich, dann 2-wöchentlich) umgestellt. Prednisolon konnte ausgeschlichen werden.

Schlussfolgerungen: Zusammenfassend liegt bei der Patientin eine Takayasu Arteriitis mit Befall der von der Aorta abgehenden Halsgefäße und der linksseitigen A. subclavia vor, welche durch Armschwäche links, einem nicht messbaren Blutdruck des linken Armes und durch Sehstörungen und Schwindel auffiel. Die immunsuppressive Therapie und vor allem chirurgische Sanierung im Sinne der Schaffung eines Ascendens-Subclavia-Bypasses konnten die Durchblutung des Gehirns über das einzige hirnversorgende Gefäß (AVS) gewährleisten und die Patientin vorerst vor neurologischen Komplikationen bewahren. Die Patientin steht lebenslänglich unter doppelter Plättchenhemmung mit Acetylsalicylsäure und Clopidogrel, ebenso ist eine langdauernde immunsuppressive Therapie (derzeit Tocilizumab 162 mg/2 Wochen) notwendig. Im weiteren Verlauf wurde zweimalig (04/20, 03/22) eine Dilatation des Bypasses durchgeführt.

6.2

Sind IgG4 wirklich wichtig?

Bond M¹, Matzneller P¹, Zandonella Callegher S¹, Dejaco C^{1,2}

¹Rheumatologie – Südtiroler Sanitätsbetrieb, Bruneck, Italien;

²Rheumatologie – Medizinische Universität Graz, Graz, Österreich

Einleitung: Ein 62-jähriger Mann ohne Begleiterkrankungen kam mit Bauchschmerzen in die Notaufnahme. Die körperliche Untersuchung war unauffällig. Die Laborwerte sind in **Tab. 1** aufgeführt. Die kontrastmittelverstärkte CT (**Abb. 1a-d**) zeigte eine Weichteilgewebsvermehrung um die thorakale und infrarenale Aorta (die den rechten Harnleiter umschloss und eine Hydronephrose verursachte); auch eine sklerosierende Pankreatitis (SP) wurde festgestellt. Das PET-CT zeigte, dass die periaortalen Veränderungen hypermetabolisch waren (SUVmax von 8). Die chirurgische Biopsie des perivaskulären Gewebes zeigte ein entzündliches Infiltrat, bestehend aus Plasmazellen (PC), Lymphozyten und storiformer Fibrose (**Abb. 1e-f**). Diese Merkmale wurden als vereinbar mit einer idiopathischen fibroinflammatorischen Erkrankung angesehen, und es wurde mit Prednison 0,7 mg/kg/Tag begonnen. Der Patient wurde dann in unsere Klinik überwiesen. Aufgrund der Assoziation von retroperitonealer Fibrose, thorakaler Periaortitis, Lymphadenopathien und SP vermuteten wir eine IgG4-assoziierte Erkrankung (IgG4-RD). Der IgG4-Serumspiegel war normal (89 mg/dL). An der Biopsie wurde eine immunhistochemische Untersuchung zum Nachweis von CD138 (einem PC-Marker) und IgG4 durchgeführt. Das Verhältnis IgG4+/CD138+ lag bei 10–20% (**Abb. 1g-h**); daher konnte die Läsion nicht als „IgG4-assoziiert“ definiert werden. Die Prednison-Therapie wurde fortgesetzt. Im 9. Monat der Behandlung zeigte das PET-CT das Verschwinden der FDG-Anreicherung.

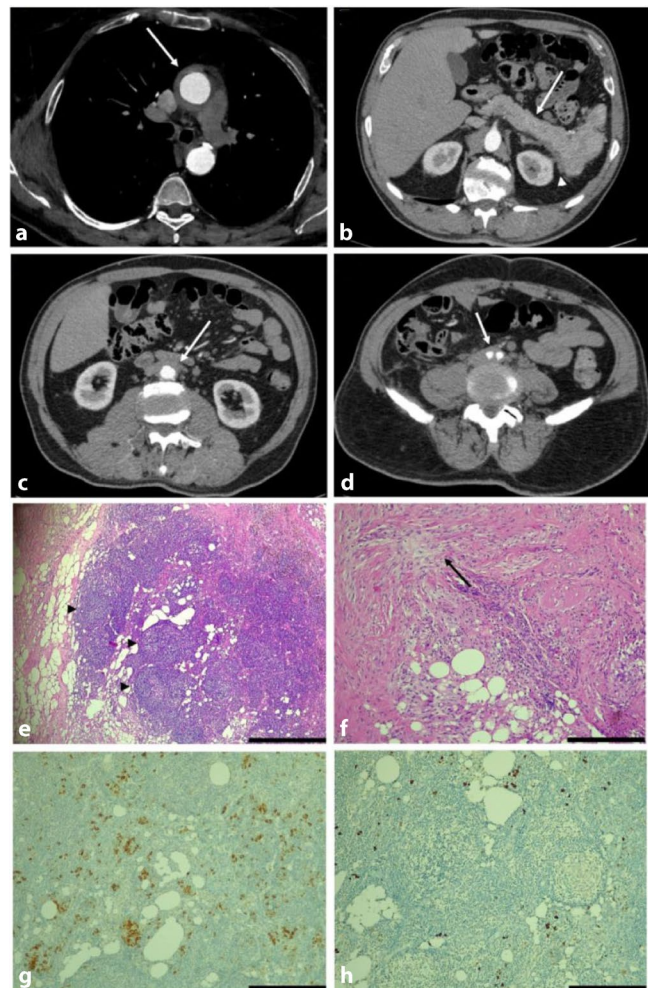


Abb. 1 | 6.2 ▲ Kontrastmittelverstärkte Computertomographie (CT) (axiale Ansicht, arterielle Phase) mit Darstellung der Aorta ascendens (**a**), umgeben von einem Ring aus weichem Gewebe (**Pfeil**), der mit einer thorakalen Periaortitis vereinbar ist. Die Bauchspeicheldrüse (**b**) erscheint abgeschwächt und wurstförmig (**Pfeil**), während sich auf ihrer Rückseite bis zum Milzhilus ein hypodenses Gewebe befindet (**Pfeilspitze**). Eine Raumforderung mit ähnlichen Merkmalen findet sich auch anterolateral der abdominalen Aorta (**c**, **Pfeil**) und der Iliakalgefäß (**d**, **Pfeil**). Die Nieren sind regulär kontrastiert, und eine Hydronephrose ist auf diesem Niveau nicht zu erkennen. Die Bilder **e–h** beziehen sich auf ein Biopsiepräparat des periaortalen Gewebes. Die Skalenbalken entsprechen 75 µm. Die Hämatoxylin-Eosin-Färbung (**e**) zeigt ein ausgeprägtes entzündliches Infiltrat mit spärlichen Keimzentren (**Pfeilspitzen**). Es sind Fibrosebänder nachweisbar (**f**), die fokal von einem Zentrum ausgehen (**Pfeil**), was dem sogenannten „storiformen“ (bastmattenähnlichen) Muster entspricht. Die CD138-Färbung (**g**) zeigt zahlreiche Plasmazellen (etwa 30/hpf), von denen bei der immunhistochemischen Analyse (**h**) etwa ein Fünftel IgG4-haltig erscheinen

Tab. 1 | 6.2 Laboruntersuchungen

Hämoglobin	11,6 g/dL
Leukozyten	8650/mm ³
Thrombozyten	164.000/mm ³
C-reaktives Protein	4,36 mg/dL
ESR	61 mm/h
Kreatinin	1,3 mg/dL
IgG4	89 mg/dL
ANA	1:80
C3 und C4	normale Werte

Schlussfolgerungen: In diesem Fall von IgG4-RD waren die IgG4 im Serum normal und die IgG4+ PC im Gewebe gering; dennoch erlaubten das radiologische Erscheinungsbild der Läsionen und die pathologischen Merkmale mit dichtem lymphoplasmozytärem Infiltrat und storiformer Fibrose eine Diagnose und Klassifizierung gemäß den ACR/EULAR-Klassifizierungskriterien 2019 für IgG4-RD. Die klinisch-radiologischen Merkmale verbesserten sich auch rasch unter Glukokortikoidtherapie, was für diese Erkrankung typisch ist. IgG4-RD ist eine idiopathische Erkrankung, die fibroinflammatorische Läsionen in fast allen Organ systemen verursacht. Eine umfassende Bildgebung ist notwendig, um eine Multiorganbeteiligung zu erkennen, und liefert Anhaltspunkte für die Beurteilung.

Abstracts

lung des Krankheitsverlaufs, während Labortests für die Fallerkennung oft wenig hilfreich sind, da Serum-IgG4 weder sensitiv noch spezifisch ist. Daher gilt die Biopsie als „Goldstandard“ für die Diagnose. Die Anzahl der IgG4+-Zellen im Gewebe übersteigt normalerweise ein IgG4+/CD138+-Verhältnis von 40 %. Es gibt jedoch auch Patienten mit typischem Organbefall, die keine IgG4-Signatur aufweisen. Bezeichnenderweise können Patienten mit einer entsprechenden klinisch-pathologischen Präsentation die 2019 ACR/EULAR-Klassifikationskriterien für IgG4-RD unabhängig von der Anzahl der IgG4+-Zellen im Gewebe erfüllen.

6.3

Ein seltsamer Fall von aseptischer Meningitis bei einer Patientin mit rheumatoider Arthritis

Zandonella Callegher S, Zampogna G, Weisseiner S, Bond M, Dejaco C

Landesweiter Dienst für Rheumatologie, Bruneck, Italien

Einleitung: Wir berichten über den Fall einer 51-jährigen Frau mit seropositiver rheumatoider Arthritis (RA), die sechs Monate nach dem Beginn einer Therapie mit Adalimumab eine aseptische Meningitis entwickelte. Die Therapie wurde im Februar 2020 begonnen und führte nach 3 Monaten zu einer klinischen Remission. Im September 2020 wurde die Patientin in die neurologische Abteilung eingeliefert, weil sie zwei kurze Episoden einer plötzlichen, selbstlimitierten rechtsseitigen Parästhesie der rechten Körperhälfte erlitt. Die neurologische Untersuchung war unauffällig. Die MRT des Gehirns zeigte ein abnormales Kontrastmittelanreicherung im linken Frontallappen (**Abb. 1a**). Die Parästhesieepisoden wurden als fokale Anfälle interpretiert, und es wurde eine antiepileptische Therapie eingeleitet. Die durchgeführte Analyse ergab keinen Hinweis auf ein infektiöses Geschehen oder eine Krebserkrankung. Aufgrund der diagnostischen Ungewissheit wurde eine pachy- als auch leptomeningeale Biopsie durchgeführt. Die präoperative MRT zeigte eine deutliche Progression der Meningitis mit diffuser meningealer Kontrastmittelanreicherung in der linken Hemisphäre. Die Histologie ergab in Folge eine chronische nekrotisierende granulomatöse Pachy- und Leptomeningitis (**Abb. 2**). Die Polymerase-Kettenreaktion war negativ für Tuberkulose und andere Mykobakterien. Es wurde die Arbeitsdiagnose einer Anti-Tumor-Nekrose-Faktor (TNF)-α-Therapie-assoziierten aseptischen Meningitis (TAAM) gestellt und Adalimumab wurde im November 2021 abgesetzt. Danach zeigte die MRT eine deutliche Verringerung der Kontrastmittelanreicherung; das Fortbestehen der Anreicherung im linken Frontallappen wurde als Folge der Operation interpretiert (**Abb. 1b, c**). Nach Beginn der antiepileptischen Therapie traten keine Anfälle mehr auf, aber wegen der anhaltenden EEG-Anomalien wurde fortgesetzt. Die Patientin wurde anschließend nur mit Methotrexat behandelt und die RA hatte eine geringe Krankheitsaktivität.

Schlussfolgerungen: Die arzneimittelinduzierte aseptische Meningitis ist eine äußerst seltene Komplikation von TNF-α-Hemmern, die einer infektiösen, insbesondere tuberkulösen Meningitis ähneln kann. Bislang wur-

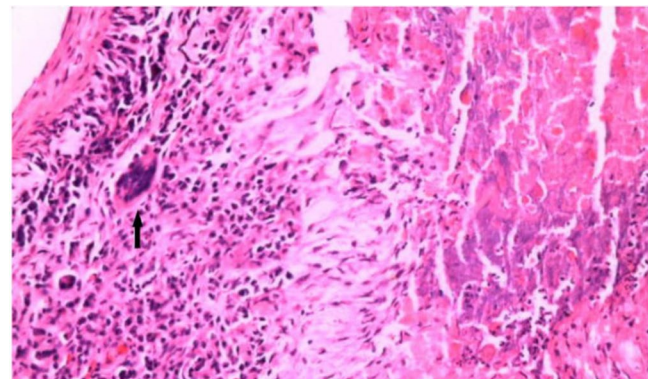


Abb. 2 | 6.3 ▲ Mikroskopische Aufnahmen der Dura Mater bei chronischer Pachymeningitis (H&E-20x): links Lymphozyten- und Plasmazelleninfiltrat mit vereinzelten vielkernigen Zellen (schwarzer Pfeil), rechts Nekrose

den nur 13 Fälle von TAAM beschrieben. Die Pathophysiologie der TAAM ist unklar. TNF-α-Hemmern können die Blut-Hirn-Schranke nicht überwinden, daher ist eine direkte toxische Wirkung unwahrscheinlich. Es wurde ein einer Typ III Überempfindlichkeitsreaktion entsprechendes Anti-Arzneimittelantikörper vermitteltes der Serumkrankheit ähnliches Syndrom postuliert. Es ist auch denkbar, dass die Granulombildung durch eine Veränderung des Zytokingleichgewichts gefördert wird. Zusammenfassend muss TAAM als mögliche Differenzialdiagnose bei Patienten die TNF-α-Hemmern, wie Adalimumab, erhalten und eine Meningitis entwickeln in Betracht gezogen werden. Das Absetzen des verursachenden Medikaments kann zum Abklingen der Meningitis führen.

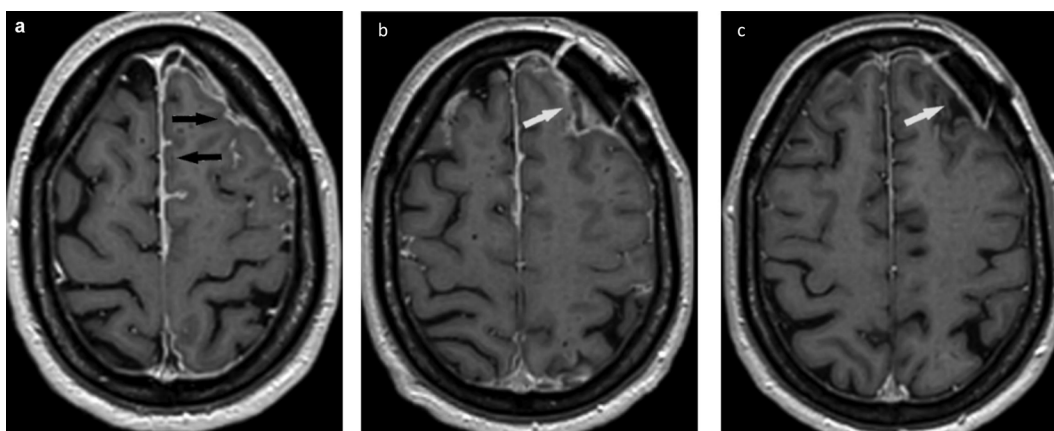
6.4

Affenpocken-assoziierte akute Arthritis

Fonti M¹, Mader T², Höpler W², Horvath-Mechtler B³, Erlacher L^{1,4}, Burmester-Kiang J¹

¹Klinik Favoriten, 2. Med. Abteilung für Rheumatologie und Osteologie, Wien, Österreich; ²Klinik Favoriten, 4. Med. Abteilung mit Infection- und Tropenmedizin, Wien, Österreich; ³Klinik Favoriten, Abteilung für Radiologie, Vienna, Österreich; ⁴Karl Landsteiner Institut for Autoimmun Diseases and Rheumatology, Wien, Österreich

Einleitung: Ein 31-jähriger Mann präsentierte sich initial mit einem vesikulären Ausschlag, perianalen Läsionen, geschwollenen Leistenlymphknoten und Schmerzen des rechten Kniegelenkes an der Abteilung für Infektiologie der Klinik Favoriten vor. An Erkrankungen war eine HIV-Infektion vorbekannt, die Viruslast war unter antiretroviraler Therapie unterhalb der Nachweisgrenze (CD4-Zellzahl 802/ μ l; Normbereich 410–1590 Zellen/ μ l). Eine Woche vor dem Auftreten der Symptome hatte



der Patient ungeschützten Geschlechtsverkehr. Aufgrund der Klinik und Anamnese wurde der Verdacht auf eine Affenpocken-Infektion gestellt. Die Diagnosesicherung der Affenpockenvirus-Infektion erfolgte durch PCR Analyse (Polymerase-Kettenreaktion) von Proben aus zwei verschiedenen Hautläsionen – („cycle threshold“, CT-Wert 20 bzw. 21). Der Patient wurde bei milder Symptomatik in die Selbstisolation entlassen. Elf Tage später, am Ende der Quarantäne, zeigte sich das Exanthem und die Lymphadenopathie vollständig abgeklungen. Auffällig war eine neu aufgetretene ausgeprägte, schmerzhafte Schwellung des rechten Kniegelenkes. Der Patient wurde daraufhin an der Abteilung für Rheumatologie und Osteologie vorstellig. Laborchemisch fanden sich, bis auf ein leicht erhöhtes C-reaktives Protein (CRP) von 18 mg/L, keine weiteren Auffälligkeiten. Die gesamte Rheumaserologie war negativ. Die Arthrosonographie zeigte einen deutlichen Gelenkerguss rechts. Mittels Arthrozentese konnten 60 ml trübe Synovialflüssigkeit gewonnen werden. Die Analyse der Synovialflüssigkeit ergab das Bild einer unspezifischen Arthritis (Zellzahl 16.127/ μ l, 88,5 % mononukleären Zellen (Lymphozyten), 11,5 % neutrophile Granulozyten). Eine ergänzende PCR Analyse des Punktats erbrachte einen positiven Nachweis des Affenpockenvirus (CT-Wert 27). Eine Magnetresonanztomographie (MRT) des rechten Kniegelenkes ergab neben einer Synovitis mit Resterguss ein ausgeprägtes Ödem des medialen Femurkondyls mit subchondraler Demarkationszone von 1 cm, dem Bild einer Osteomyelitis entsprechend. Eine symptomatische Therapie mit nichtsteroidalen Antirheumatischen (NSAR) wurde etabliert. Darunter kam es innerhalb von drei Wochen zu einer deutlichen Verbesserung der Arthralgien und einem Rückgang der Gelenksschwellung.

Schlussfolgerungen: In der Literatur finden sich Nachweise des Affenpockenvirus in Nasen-Rachen-Abstrichen, aus Haut- und Schleimhautläsionen, Sperma, Speichel, Urin, Stuhl und direkt aus Blutproben. Dies ist der erste dokumentierte direkte Virusnachweis aus Synovialflüssigkeit und stellt somit die erste Beschreibung einer Affenpocken-assoziierten akuten Arthritis dar. Viren sind, nach Bakterien, häufige Auslöser von infektiösen Arthritiden, jedoch ist das Auftreten einer viralen Osteomyelitis eine Rarität. Speziell bei Pockeninfektionen ist das Auftreten der sogenannten Osteomyelitis variolosa eine bekannte Komplikation und wird in der Literatur mit einer Prävalenz von 2–5 % der infizierten Kinder und 0,25–0,5 % aller mit Pocken infizierten PatientInnen angegeben. In Anbetracht der Tatsache, dass das Variola-Virus und das Affenpocken-Virus eng miteinander verwandt sind, beide aus der Familie der Orthopoxviren, kann eine virale Osteomyelitis als Ursache der Knochenläsionen im aktuellen Fall angenommen werden.

6.5

Pancreatitis-Panniculitis-Polyarthritis-Syndrome—a hidden diagnosis—case report

Storch K¹, Bécéde M¹, Krampf W², Trautinger F³, Mayer A⁴, Sautner J¹

^{1,2} Medizinische Abteilung, NÖ Kompetenzzentrum für Rheumatologie, Stockerau, Austria; ²Institut für Radiologie, Landesklinikum Stockerau, Stockerau, Austria; ³Klinische Abteilung für Haut- und Geschlechtskrankheiten, Universitätsklinikum St.Pölten, St.Pölten, Austria;

⁴Abteilung für Innere Medizin 2, Universitätsklinikum St.Pölten, St.Pölten, Austria

Introduction: PPP—the combination of pancreatitis, panniculitis and polyarthritis is a rare, systemic syndrome that occurs in patients with acute or chronic pancreatitis or pancreatic malignancies. The early detection of this triad, especially in patients without any indicating abdominal symptoms, can avoid delays in specific diagnostic steps and therapy. A 50-year-old male patient presented with increasing joint pain and polyarthralgia in wrists and ankles for one week, impairing his ability to walk without additional aids for three days. The physical examination showed isolated nodules on the lower extremities on the extensor, as well as the flexor sides without any tenderness to pressure (Fig. 1), also the patient presented with multiple swollen joints (polyarthritis). Laboratory tests showed elevated pancreatic enzymes. Pancreatitis was assumed and verified by abdominal CT-scan, showing signs of chronic pancreatitis with concretions in the pancreatic duct. The diagnosis of panniculitis was confirmed by dermatological consultation. Concerning pancreatitis and panniculitis, the patient was hardly affected. In accordance to pre-existing literature, oral glucocorticoid therapy and NSAIDs failed to improve pain or polyarthralgia. Endosonography showed signs of chronic pancreatitis with calcifications, as well as acute inflammation of the pancreatic head. Subsequently ERCP was performed, the pancreatic duct was dilated, concretions were removed and a stent was implanted. Following ERCP, an instant decrease of pancreatic enzymes was observed, accompanied by a clear and sustained improvement of given polyarthritis.



Abb. 1 | 6.4 ▲ Knieschwellung (a), Haut Läsion (b), MRT des Knies mit subchondraler Demarkationszone und Erguss (c–e)



Fig. 1 | 6.5 ▲ Panniculitis of the lower limbs

Abstracts

Conclusion: The typical triad of clinical findings in mind, one should consider the PPP-syndrome in the context of acute or chronic pancreatitis. Panniculitis is often confused with erythema nodosum, which can lead to diagnostic delays and incorrect therapy. Regarding PPP, arthritis is usually chronic and responds poorly to NSAIDs or corticosteroids. A rare, but dreaded complication is a sudden increase in swelling of joints, leading to perforation and necrosis within a few days, requiring necrosectomy, incision, and debridement on all four limbs. All involved disciplines (gastroenterology, dermatology and rheumatology) should be familiar with this rare but severe condition. The prognosis depends on the extent of functional deficit of the extremities and the progression of pancreatitis.

Hinweis des Verlags. Der Verlag bleibt in Hinblick auf geografische Zuordnungen und Gebietsbezeichnungen in veröffentlichten Karten und Institutsadressen neutral.

Autorenverzeichnis

A

- Agostino M. 2.12
 Akbari K. 2.1
 Alasti F. 2.11
 Aletaha D. 1.1, 2.10, 2.11, 2.13

B

- Backhaus M. 2.12
 Balint PV. 2.12
 Bécède M. 2.4, 6.5
 Berner Hammer H. 2.12
 Blessberger H. 2.8
 Bond M. 6.2, 6.3
 Bonelli M. 1.1
 Bong D. 2.12
 Bosch P. 1.2, 1.3, 2.9, 5.3
 Brezinsek H. 1.4, 1.5
 Buchmann A. 1.3
 Burmester-Kiang J. 6.4

C

- Cipolletta E. 2.12
 Collado P. 2.12
 Cor nec D. 2.3

D

- de Thurah A. 2.9
 de Wit M. 2.11
 Deimel T. 2.10, 2.13
 Dejaco C. 2.10, 2.12, 2.9, 5.3, 6.2, 6.3
 Delle Sodie A. 2.12
 Dellinger M. 1.1
 Dreß B. 1.2, 1.3, 1.5, 2.2, 2.3, 5.1
 Duftner C. 2.12
 Durechova M. 2.13

E

- Eichbauer-Sturm G. 2.7
 ein Fallbericht 3.2
 Emminger W. 6.1
 Erlacher L. 2.3, 6.4

F

- Falzon L. 2.9
 Fasching P. 5.1
 Felson DT. 2.11
 Ferincz V. 2.7
 Fessler J. 1.2, 1.3, 2.2, 2.5, 5.1
 Filippou G. 2.12
 Filippucci E. 2.12
 Fonti M. 6.4
 Fritsch-Stork im. 2.7

G

- Gessl I. 2.10, 2.12, 2.13
 Girschick H. 3.1
 Grösch N. 3.1

H

- Hana C. 2.13
 Hayer S. 5.1
 Heinz L. 1.1
 Helmberg W. 5.1
 Herbstrofer L. 1.4
 Hermann J. 2.10, 2.5, 2.6
 Herold M. 2.7
 Heubner G. 3.1
 Hintenberger R. 2.1, 2.8
 Hodl I. 2.2
 Hojreh A. 6.1
 Höpler W. 6.4
 Horner A. 2.1
 Horvath-Mechtler B. 6.4
 Hospach T. 3.1
 Hucke M. 2.13
 Husic R. 1.2, 1.3, 2.10

I

- Iagnocco A. 2.12

J

- Javorova P. 2.3
 Johannes W.J. 2.9

K

- Karim Z. 2.12
 Karonitsch T. 1.1
 Kartnig F. 1.1
 Keen H. 2.12
 Khalil M. 1.3
 Kickinger D. 5.3
 Kiener H. 1.1
 Kitzmüller E. 6.1
 Klotsche J. 3.1
 Kofler S. 1.5
 Konzett V. 2.13
 Krampala W. 6.5
 Kreuzer S. 1.5
 Kugler M. 1.1

L

- Lacaille D. 2.11
 Lackner A. 1.2, 1.3, 2.10, 2.2, 2.3, 2.5,
 2.6, 5.1
 Lamprecht B. 2.1
 Lang D. 2.1, 2.8
 Leeb B. 2.7
 Lopez-Garcia P. 1.4

M

- Mader T. 6.4
 Mandl P. 2.10, 2.12, 2.13
 Marques A. 2.9
 Matzneller P. 6.2
 Mayer A. 6.5
 Meissner Y. 2.9
 Minden K. 3.1
 Moazedi-Fürst F. 1.5, 2.2
 Möller I. 2.12
 Mukhtyar C. 2.9
 Müller L. 1.1
 Mur E. 4.1
 Muralikrishnan AS. 1.2, 1.3

N

- Naredo E. 2.12
 Niederwirth M. 3.1

O

- Orazio M. 1.5, 2.3

P

- Pfeifer V. 1.4, 1.5
 Pieber T. 1.4
 Pieringer H. 2.8
 Pietsch DR. 1.2
 Pineda C. 2.12
 Popescu M. 2.13
 Preglej T. 1.1
 Prietl B. 1.4, 1.5
 Puchner R. 2.7, 2.8, 5.3

R

- Reisch M. 5.3
 Reiser C. 3.1
 Resch-Passini J. 2.7
 Rintelen B. 2.7
 Rupp J. 1.2, 1.3, 5.1

S

- Sallegger C. 2.2
 Sanz A. 2.6
 Sautner J. 2.4, 2.8, 6.5
 Sautner T. 2.4
 Schlenke P. 5.1
 Schmidt W. 2.12
 Schwantzer G. 2.10
 Shao G. 2.1
 Sirotti S. 2.12
 Smolen J. 2.10
 Smolen JS. 2.11, 2.13
 Sourij H. 1.5
 Spellitz P. 2.7
 stamm T. 2.9

Autorenverzeichnis

Stamm TA.	2.11
Steiner G.	1.1, 5.1
Stetter M.	2.7
Storch K.	2.4, 6.5
Stradner M.	1.4, 2.10, 2.2
Stradner MH.	1.2, 1.3, 1.5, 2.3, 2.5, 2.6, 5.1
Studenic P.	2.11, 2.13
Stummvoll G.	4.1
Supp G.	2.10, 2.13
Szkudlarek M.	2.12

T

Tamborini G.	2.12
Terslev L.	2.12
Thiel J.	1.2, 1.3, 1.5, 2.2, 2.3, 2.5, 2.6, 5.1
Tosevska A.	1.1
Trautinger F.	6.5
Trauzeddel R.	3.1

U

Ukalovic D.	2.7
Ulbrich A.	6.1

V

Valent I.	6.1
Veitl M.	2.4
Vera-Ramos J.	1.4

W

Wegscheider C.	5.2
Weissteiner S.	6.3
Weyand CM.	5.1
Wiederer C.	4.1
Windisch E.	2.3
Windschall D.	3.1
Winkler F.	2.4
Winkler S.	2.4
Wong P.	2.12

Z

Zampogna G.	6.3
Zandonella	
Callegher S.	6.2, 6.3
Zauner M.	2.13
Zenz S.	1.5, 2.3, 2.5, 2.6
Zimmermann-	
Rittreiser M.	2.7
Zimpfer D.	6.1